

Synchrotron Microtomographic Osteology of the Chinese Subterranean Catfish: Description and Systematic Analysis

Y. He^a, *, J. G. Lundberg^b, **, J. Yang^c, ***, and J. X. Yang^d, ****

^a Shanghai Synchrotron Radiation Facility, Shanghai Advanced Research Institute, Chinese Academy of Sciences, Shanghai, China

^b Department of Ichthyology, Academy of Natural Sciences, Philadelphia, USA

^c Key Laboratory of Beibu Gulf Environment Change and Resources Use, Nanning Normal University, Nanning, China

^d State Key Laboratory of Genetic Resources and Evolution, Kunming Institute of Zoology, Chinese Academy of Sciences, Kunming, China

*e-mail: heyou@sinap.ac.cn

**e-mail: jgl43@drexel.edu

***e-mail: yj1981yj@163.com

****e-mail: yangjx@mail.kiz.ac.cn

Received June 25, 2024; revised September 17, 2024; accepted September 24, 2024

Abstract—We use synchrotron microtomography to study the osteology of an eyeless stygobitic catfish from South China with the objective of examining its systematic position. The results support to assign this species to the superfamily Sisoroidea. *Proliobagrus* He, Lundberg, Yang et Yang, gen. nov. is proposed diagnosed with a combination of characters: infraorbital bones reduced to one posteriormost element and lacrimal; mesocoracoid arch incomplete; first dorsal-fin pterygiophore compressed lacking paired bony canals for erector muscles, fused with an anteriorly directed process at its proximal end, and remote from Weberian complex; compound Weberian centrum with a ventral median ridge instead of paired ventrolateral ridges, an auxillary parapophysis posterolaterally off compound Weberian centrum, heavy strut-like process ventrally off the fourth neural spine, claustrum absent, tripus with outwardly extended transformator process; anterior cranial fontanelle closed, posterior cranial fontanelle subdivided into anterior and posterior remnant; first proximal pectoral-fin radial roughly round; dorsal and ventral procurrent caudal-fin rays less than ten respectively; base of nasal barbel on anterior rim of posterior nostril; skin lacking tubercles. In a first cladistic analysis, *Proliobagrus* is grouped with sampled amblycipitid species. The abrupt change of insert position of the first dorsal-fin pterygoid implies that none of extant amblycipitid species could be considered as direct ancestor of *Proliobagrus* and it represents a relic lineage surviving in subterranean waters.

Keywords: cave fish, South China, *Proliobagrus*, Amblycipitidae, Sisoroidea

DOI: 10.1134/S0032945224701017

INTRODUCTION

Freshwater fishes can explore the subterranean waters as their habitats. Some are tentatively visitors to groundwater or represent a hypogean population of surface species, whereas others have survived in dark groundwaters over geological time and their close surface relatives might have been extinct. Catfishes (Order Siluriformes), along with cypriniforms, are a dominant group of subterranean fishes (Romero and Paulson, 2001; Proudlove, 2010). In contrast to the rich diversity of subterranean cyprinids and loaches in karst aquifers of southwest China, Southeast Asia and Indian subcontinent, there are few stygobitic (obligate aquatic cave-dwelling) catfish. Out of more than 55 hypogean catfishes in 10 families (Proudlove, 2010), only 8 species (4 genera in 4 families) are known

in Asia: *Horaglanis krishnai* Menon, 1951, *H. alikunhii* Babu and Nayar, 2004, *H. abdulkalami* Babu, 2012 and *H. populi* Raghavan, Sundar, Arjun, Britz, Dahanukar, 2023 from India, *Kryptoglanis shajii* Vincent and Thomas, 2011 from India, *Pterocryptis buccata* Ng and Kottelat, 1998, and *P. cucphuongensis* Ng and Kottelat, 1998 from Thailand and Vietnam, *Xiurenbagrus dorsalis* Xiu, Yang and Zheng, 2014 from China. The cave-dwelling *Pterocryptis* species are recognized as the hypogean population of the conspecific surface species (Ng and Kottelat, 1998a), whereas *Horaglanis* and *Kryptoglanis* cavefishes are relict lineages with their phylogenetic positions yet unresolved (Britz et al., 2014; Lundberg et al., 2014; Britz et al., 2019). *Kryptoglanis* has been assigned to its own family (Britz et al., 2014). The Chinese cave catfish *Xiurenbagrus dorsalis*, currently assigned to the Amblycipitidae, is

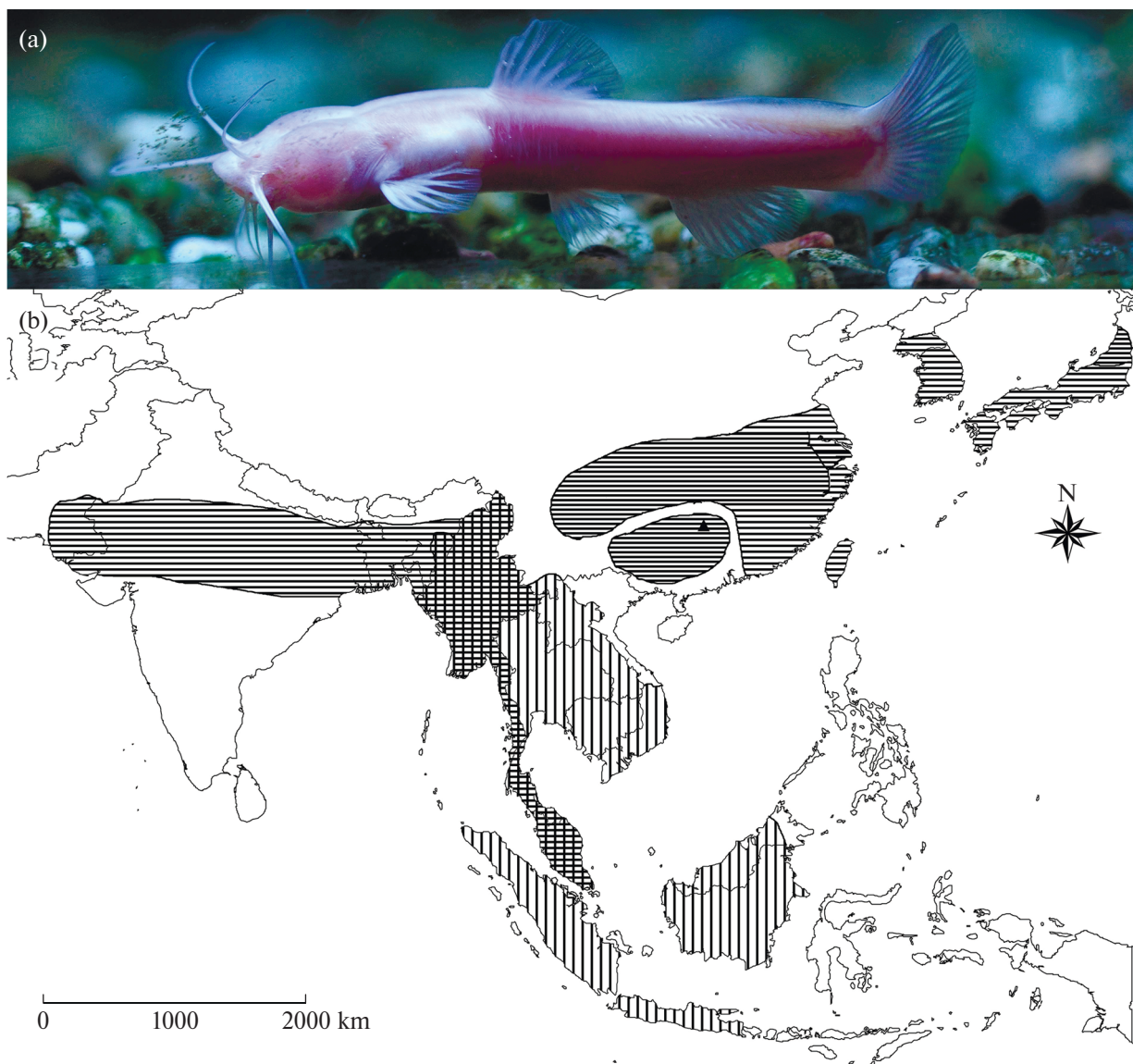


Fig. 1. A living *Proliobagrus* (*Xiurenbagrus*) *dorsalis* (a) (photo by L.A. Ouyang), type locality of *P. dorsalis* (▲) and geographic distribution of the families Amblycipitidae (▨) and Akysidae (▨▨) (b).

eyeless and translucent with a long nasal barbel, a posteriorly placed dorsal fin and an adipose fin confluent with the caudal fin (Figs. 1a, 2a). Given its superficial resemblance to amblycipitids and the presence of vomerine teeth, Xiu et al. (2014) assigned this species to the amblycipitid genus *Xiurenbagrus*. The holotype was collected from an artificial well in 2011 in south China (Xiu et al., 2014), where two specimens were caught and photographed on 10 Jan 2015 from the vicinity of type locality (Fig. 1a; fish was released after photographing L.A. Ouyang, pers. comm.). However, neither osteological study nor molecular investigation of this cave catfish has been performed, and its close surface relatives remain unknown.

X-ray microtomography has been widely used to reveal internal three-dimensional anatomic details at micron resolution in a non-destructive way, and a lot of skeletons of various catfishes has been successfully reconstructed and described around world based on this approach (Schaefer, 2003; Devaere et al., 2005; Rodiles-Hernandez et al., 2005; Lundberg et al., 2014; Carvalho et al., 2017; de Pinna and Keith, 2019; and others). As for subterranean fishes, the authors have applied X-ray microtomography to revealing the systematic position of spine loach in combination with molecular phylogeny (He et al., 2021), the skeleton of several hypogean catfishes (Lundberg et al., 2014, 2017), the skeleton features of hypogean goby (He et al., 2015), and adaptive characters related to subter-

ranean life of cave carp (He et al., 2013). The aims of this study are first to describe and illustrate in detail the osteological, cartilaginous, and key external morphological characters of the holotype of this species using synchrotron X-ray microtomography; second, to investigate the systematic position by comparing this stygobitic species within the Asian superfamily Sisoroidea in relation to the “Big Asia clade” of Sullivan et al. (2006). The results of a first cladistic analysis of this catfish among the Sisoroidea presented herein. The previously proposed synapomorphies of the Amblycipitidae (Chen, 1994) were reviewed.

MATERIALS AND METHODS

Materials

Collection abbreviations follow Sabaj (2020): ANSP, The Academy of Natural Sciences of Philadelphia, USA; AUM, Auburn University Museum of Natural History, USA; CAS, California Academy of Sciences, USA; GIF, Guangxi Institute of Fisheries, China; IHB, Institute of Hydrobiology, Chinese Academy of Sciences, China; KIZ, Kunming Institute of Zoology, Chinese Academy of Sciences, China; KU, University of Kansas, USA; SAIAB, South African Institute for Aquatic Biodiversity, South African; SWU, Southwest University, China; UF, University of Florida, USA; YU, Yunnan University, China. Some specimens are personal preserved by Mr. Jiahu Lan (LJH).

Xiurenbagrus dorsalis, holotype, GIF 2011050901 (49 mm standard length, collected in May 2011). The comparative materials include the representatives from the superfamily Sisoroidea, and other members of the Big Asia clade. They are listed as the following. **Akysidae**: *Akysis vespa*, KIZ 3474, KIZ 3473; **Acrochordonichthys rugosus*, UF:FISH:167005; **Pseudobagarius hardmani*, ANSP:FISH:178858. **Amblycipitidae**: *Amblyceps Yunnanensis* KIZ 20220361, KIZ 20220362; *Liobagrus anguillicauda*, IHB 201111001, IHB 201111004; *Liobagrus sp.* LJH unnumbered; *Xiurenbagrus gigas*, LJH 02040108, LJH 02040106; *Xiurenbagrus xiurensis*, LJH 02050849, LJH 02050827; LJH 02050832. **Sisoridae**: **Ayarnangra estuaries*, ANSP:FISH:205752; **Bagarius yarrelli*, UF:FISH:185219; **Gagata dolichonema*, AUM:FISH:55782; **Glyptothorax buchanani*, UF:FISH:191340; **Glyptothorax trilineatus*, UF:FISH:192385; *Glyptosternum maculatum*, SWU 201909010179, SWU 201909020213; **Nangra nangra*, KU:KUI:29508; *Pareuchiloglanis longicauda*, YU unnumbered; *Pareuchiloglanis anteanalisis*, YU unnumbered; *Pseudecheneis sulcatus*, YU 3569; **Pseudecheneis sulcate*, KU:KUI:40671; *Pseudecheneis sulcatoidea*, YU 0902044; **Pseudolaguvia kapuri*, CAS:ICH:50294; *Oreoglanis delacouri*, YU 20100514024; **Oreoglanis siamensis*, AUM:FISH:55729; and the skeletal preparations Chi-

marrichthys davidi, KIZ 795579; *Glyptothorax fukiensis*, KIZ 733031, KIZ 200304004; *Pareuchiloglanis anteanalisis*, KIZ 20040620001; *Pareuchiloglanis gracilicaudata*, KIZ 20040929008; *Pareuchiloglanis macrotremia*, KIZ 2000051121; *Pseudexostoma yunnanense*, KIZ 2008006; *Pseudexostoma brachysoma*, KIZ 764121; *Oreoglanis jingdongensis*, KIZ 200104005; *Oreoglanis macropterus*, KIZ 740154; *Oreoglanis immaculatus*, KIZ 200261017, KIZ 200261018; *Oreoglanis insignis*, KIZ 764025, KIZ 764447. **Bagridae**: *Leiocassis longirostris*, SWU unnumbered (artificial bred); *Hemibagrus macropterus*, SWU unnumbered (artificial bred); *Hemibagrus nemurus*, *AUM:FISH:55366; *Mystus gulio*, *UF:FISH:161553. **Horabagridae**: *Horabagrus brachysoma*, *SAIAB:FISH:59825. **family incertae sedis**: *Laides hexanema*, *UF:FISH:165965; *Rita rita*, *KU:FISH:29116. **Diplomystidae**: **Diplomystes chilensis*, KU:KUI:19255. The species labelled with star are micromorphographic skeletons from www.MorphoSource.org.

X-Ray Microtomography

The synchrotron radiation X-ray microtomography (SR- μ CT) was used to image *Xiurenbagrus dorsalis* (GIF 2011050901) at BL13W1 beamline of the Shanghai Synchrotron Radiation Facility, Shanghai, China. The specimen was vertically held in a plastic tube filled with 90% ethanol solution, mounted on the sample stage and imaged by 18.0 keV monochromatic X-ray at the final 5.2 μ m pixel resolution. The imaging parameters were referred to a previous protocol (He et al., 2016). As the vertical size of the synchrotron X-ray beam (about 5 mm) is far less than the body length, the specimen was vertically moved 4.0 mm after scanning one 4.0 mm segment to allow the consecutive scanning for the whole specimen. *Akysis vespa* (KIZ 3474; KIZ 3473), *Liobagrus sp.* (LJH unnumbered), *Liobagrus anguillicauda* (IHB 201111001; IHB 201111004), *Pareuchiloglanis longicauda* (YU unnumbered), *Pareuchiloglanis anteanalisis* (YU unnumbered), *Pseudecheneis sulcatus* (YU 3569), *Pseudecheneis sulcatoidea* (YU 0902044), *Oreoglanis delacouri* (YU 20100514024), and *Xiurenbagrus gigas* (LJH 02040108, LJH 02040106) were scanned using MicroCT Skyscan 1176 (Bruker, Belgium) with 50 kV tube voltage, 0.3-degree rotation step and 9 μ m voxel size. *Xiurenbagrus xiurensis* (LJH 02050849, LJH 02050827, LJH 02050832) was also scanned, but failed to get the skeleton due to the decalcification of the specimens. The cross-sections were reconstructed using the software attached to the MicroCT scanner. Micromorphographic skeletons of other species, labeled with star in the comparative materials, are downloaded from MorphoSource.org. The three-dimensional renderings were created, visualized and manipulated in the VG Studio Max (v2.1) software. By increasing the grey value threshold, bones and soft-tissue (cartilage, muscles)

were easily distinguished, as the bones remained while the soft tissues were virtually removed (He et al., 2013).

Terminology for osteological structures follows Lundberg et al. (2017), except for using lacrimal instead of the first infraorbital, coracoid instead of scapulocoracoid, supracleithrum instead of posttemporo-supracleithrum, following Kubicek (2022).

Phylogenetic Framework and Cladistic Analysis

The family Amblycipitidae currently consists of three genera inhabiting eastern, southeastern, and southern Asia (Fig. 1b): *Amblyceps* Blyth 1858, *Liobagrus* Hilgendorf 1878, and *Xiurenbagrus* Chen and Lundberg 1995. Among siluriforms, the Amblycipitidae is most closely related to the Akysidae and Sisoridae (Chen, 1994; Friel, 1994; de Pinna, 1996; Diogo, 2005; Sullivan et al., 2006; Ng, 2010).

De Pinna (1996) was the first to propose the superfamily Sisoroidea comprising the Asian families Akysidae, Amblycipitidae, Erethistidae (now a subgroup of Sisoridae), Sisoridae, and the South American family Aspredinidae in which the Amblycipitidae was placed as the sister group of all other family-level clades. But there is consistent morphological evidence (Friel, 1994) and ample robust molecular evidence (Sullivan et al., 2006, 2008) supporting the Aspredinidae as most closely related to the South American Doradoidea (Doradidae and Auchenipteridae, including Ageneiosidae). Sullivan et al. (2006) were the first to indicate that the Asian families Akysidae, Amblycipitidae and Sisoridae form a monophyletic clade which, together with the Bagridae, Horabagridae, and two species *Ailia coila*, *Laides hexanema* to form an informally-named “Big Asia” clade in their molecular phylogenetic analysis of Siluriformes. Thus, the superfamily Sisoroidea is considered as a monophyletic group comprising three Asian families in the most recent phylogenetic study of the Siluriformes (Lundberg et al., 2014). It is worth noting that the molecular study challenged the previously proposed monophyly of the Amblycipitidae from morphological data (Chen, 1994).

Comparative osteological evidence (see results and discussions below) demonstrates that eyeless stygobitic catfish “*Xiurenbagrus*” *dorsalis* can be assigned with reasonable certainty to the Asian superfamily Sisoroidea (sensu Sullivan et al., 2008). The aim of cladistic analysis is to explore potential phylogenetic position of this Chinese stygobitic catfish within the Sisoroidea. Unfortunately, phylogenetic relationships within the Sisoroidea remain unresolved despite studies using molecular (Sullivan et al., 2006, 2008; Ng and Jiang, 2015) and morphological evidence studies of the Amblycipitidae (Chen, 1994) and the Sisoridae (Ng, 2010, 2015). A systematic skeletal investigation of the Akysidae has not been done and few anatomical

illustrations are available. We compiled a data matrix including 68 characters (all of which are osteological except one related on the shape of swim bladder) for 29 taxa (four species representing three genera in the Amblycipitidae, three species representing three genera in the Akysidae, 13 species representing in 12 genera the Sisoridae) (Supplement 1). The characters used in the analyses are based on the microtomographic data generated by ourselves or downloaded from MorphoSource. They are related to the features of neurocranium, splanchnocranum, Weberian apparatus and vertebrae, median and paired fins and supports, and cephalic canal system. 19 of the characters were originally adopted/modified from de Pinna (1996), three from Diogo (2005), three from Chen (1994). The species from the Diplomystidae, Bagridae and Horabagridae and *Rita rita*, *Laides hexanema* are used as the outgroup, as the Diplomystidae is the most basal lineage in siluroidei, the characters of which are supposed as plesiomorphic, and the other taxa are suggested as the close relatives to the superfamily Sisoroidea (Sullivan et al., 2006). The previous illustrations of *Amblyceps mangois* (Tilak, 1967) and of *Sisor rhabdophorus* (Mahajan, 1966, 1967) were used as reference due to the low resolution of their microCT data.

This matrix was subsequently analysed using PAUP* 4.0b8 (Swofford, 1999) and WINCLADA 1.00.08 (Nixon, 2002). Maximum parsimony analyses were performed with a heuristic search in PAUP* v.4.0b10 using 500 random addition sequence replicates, holding five trees at each step, with the tree bisection and reconnection strategy enabled and max-trees set to automatically increase by 100. Bremer support indices for the nodes were calculated using TreeRot v2c. Bootstrap values were calculated in PAUP* v.4.0b10 using 500 replicates of a heuristic search, with five trees held at each step, rearllimit = 50000000, limitperrep = yes, nchuck = 10000, chuck-score = 1.

RESULTS

As shown in the following, the Chinese eyeless stygobitic catfish species treated herein belongs to the Asian superfamily Sisoroidea. We place our new taxonomic names and diagnoses in advance of the description of morphology and the phylogenetic analysis for convenience in presenting taxonomic comparisons.

Proliobagrus He, Lundberg, Yang et Yang, gen. nov.

Figs. 2–13

Type species. *Proliobagrus dorsalis* (Xiu, Yang and Zheng, 2014). *Xiurenbagrus dorsalis* Xiu, Yang and Zheng, 2014.

Diagnosis. *Proliobagrus* is distinguished from all other sisoroids by the following combination of characters: infraorbital bones reduced to one posterior-

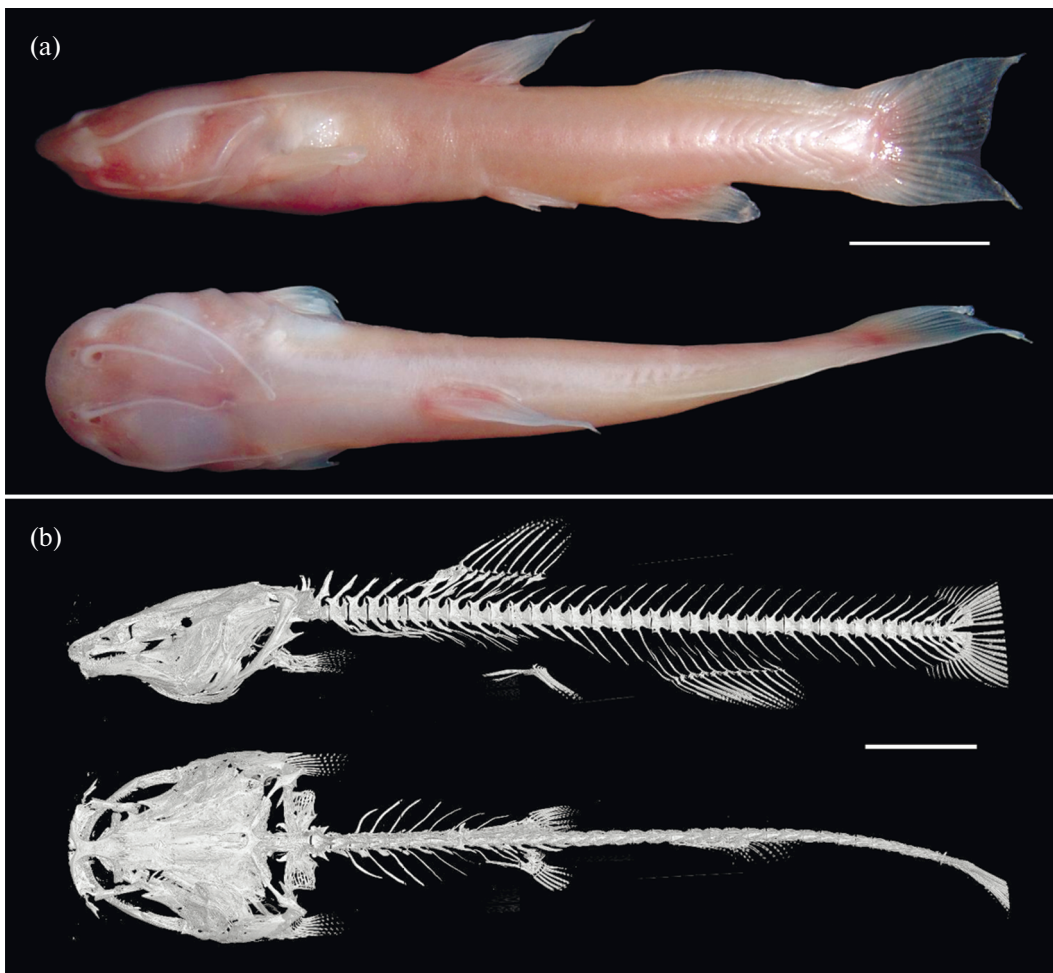


Fig. 2. *Proliobagrus dorsalis*, holotype, GIF 2011050901 (a) and overall morphology (b): overall skeleton. Scale: (a) 10, (b) 6 mm.

most element and lacrimal; mesocoracoid arch incomplete; first dorsal-fin pterygiophore compressed lacking paired bony canal for erector muscles, anteriorly fused with a forward process, and remote from Weberian complex; compound Weberian centrum with a ventral median ridge instead of paired ventrolateral ridges, an auxillary parapophysis posterolaterally off compound Weberian centrum, fourth neural spine with heavy strut-like ventral process (i.e. each half of fourth neural spine dorsoventrally bifurcated), claustrum absent, scaphium with lack of ascending process, tripus with outwardly extended transformator process; anterior cranial fontanelle closed, posterior cranial fontanelle subdivided into an aperture-like anterior and a large posterior remnants; first proximal pectoral radial roughly round; dorsal and ventral procurrent caudal-fin rays less than ten respectively; base of nasal barbel on anterior rim of posterior nostril; skin smooth with lacking tubercles.

Other characters useful for identification. Eyes absent; pigmentation absent; dorsal-fin origin posterior to and far from the tip of pectoral fin (Fig. 2a);

first dorsal spinelet absent; body depth uniform from head to caudal fin; adipose fin confluent with caudal fin (Fig. 2a); four pairs of barbels; nasal barbel longer than mental barbels, reaching occiput; maxillary barbel long, reaching tip of pectoral fin (Fig. 2a); anteriormost dorsal procurrent caudal-fin ray placed between tips of neural spines of preural centra 4 and 5, and anterior most ventral procurrent ray placed between the tips of haemal spines of preural centra 5 and 6.

Etymology. From the Latin *pro* in the sense of before, plus *Liobagrus*, an existing generic name for a group of amblycipitid catfishes inhabiting East Asia. Gender masculine.

Description

Neurocranium (Fig. 3). The neurocranium is dorsoventrally depressed, 1.65 times longer than its wide (Fig. 3a).

The mesethmoid is slender with a narrow neck and divergent anterior cornua, tapering and distally

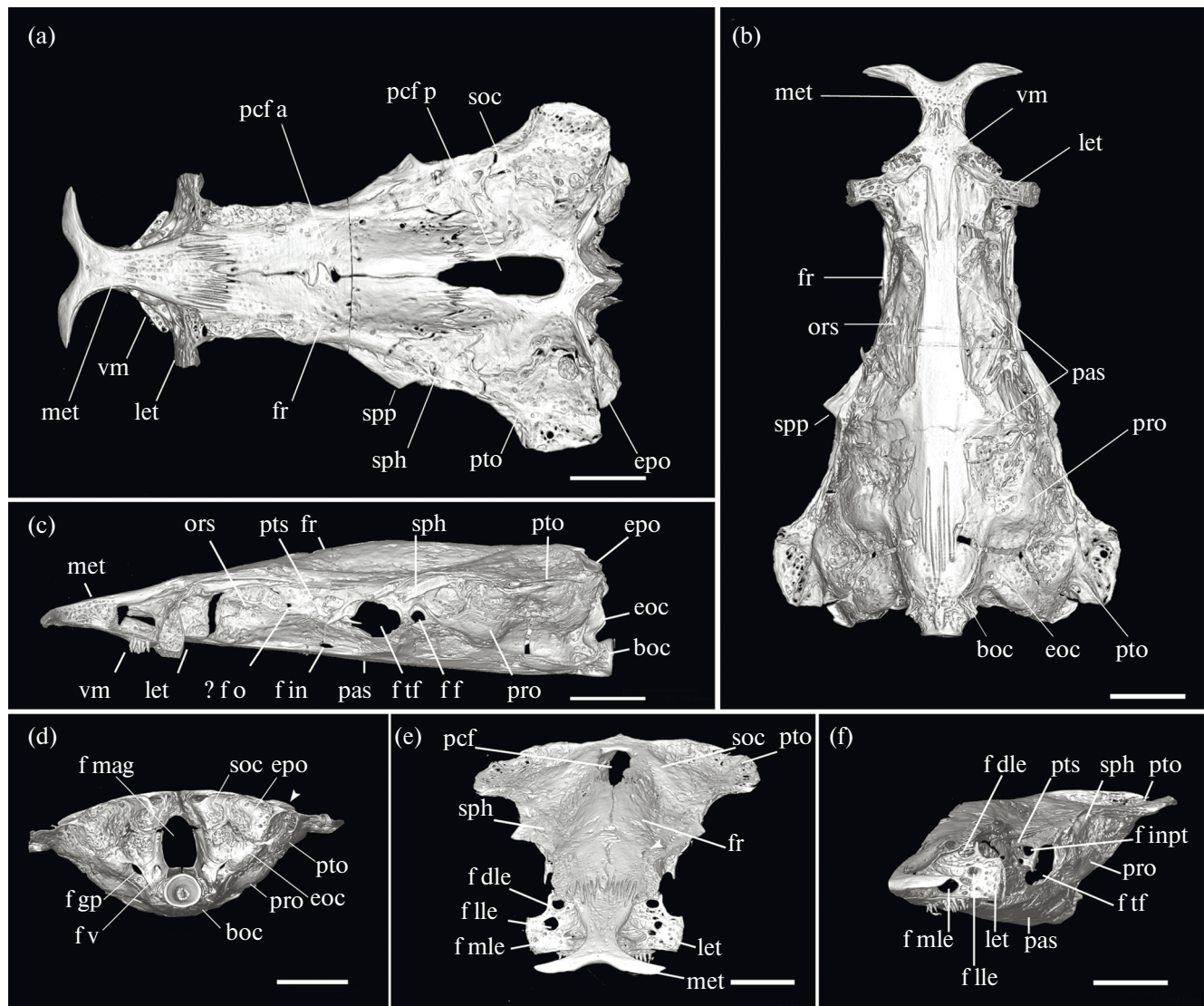


Fig. 3. Neurocranium of *Proliobagrus dorsalis*, holotype, GIFT 2011050901: (a) dorsal view, (b) ventral view, (c) lateral view, anterior to left; (d) posterior view, (e) anterior-oblique view, (f) lateral-oblique view with the right half neurocranium removed. boc, basioccipital; epo, epioccipital; eoc, exoccipital; f dle, dorsal foramen in lateral ethmoid; ff, foramen for facial nerve; fin, foramen indeterminate; f inpt, foramen indeterminate in pterygopharyngeal; fr, frontal; f lle, lateral foramen in lateral ethmoid; f mag, foramen for glossopharyngeal nerve; fo, foramen for optic nerve; f tf, foramen for trigeminal nerve; f gp, foramen for glossopharyngeal nerve; fv, foramen for vagus nerve; let, lateral ethmoid; met, mesethmoid; ors, orbitosphenoid; pas, parasphenoid; pcf a, anterior remnant of posterior cranial fontanelle; pcf p, posterior subdivision of posterior cranial fontanelle; pro, prootic; pto, pterotic; pts, pterygopharyngeal; sph, sphenotic; spp, sphenotic process; soc, supraoccipital; vm, vomer. (◀) the articular facet in epioccipital for the upper arm of the supracleithrum in (d). Scale: 1.5 mm.

pointed, and the median cleft between the cornua is shallowly concave (Figs. 3a, 4a). The mesethmoid sutures posteriorly with the paired frontals (Fig. 3a) and articulates ventrally with the dorsal surface of the premaxilla (Fig. 4a). The nasal is a weakly ossified tubular bone bearing sensory canal with three foramina, lying along the mesethmoid neck (only visible in the rendering with low grey-value threshold in Figs. 11a, 11b). The lateral ethmoid projects off the mesethmoid with a straight antorbital process, thickly cylindrical to its synchondral articulation with autopalaean central

condyle (Fig. 4a). Three foramina pierce the lateral ethmoid (Figs. 3e, 3f): a ventromedial olfactory nerve foramen nearest the mesethmoid wall; a centrally-placed orbital foramen of deep ophthalmic ramus through the base of the antorbital process, and a dorso-lateral superficial ophthalmic ramus foramen adjacent to the lateral ethmoid-frontal joint. The skull roof comprises the frontal, sphenotic, pterygopharyngeal, and occipital. The paired frontals meet medially in a simple, non-interlocking bony butt-joint closing anterior cranial fontanelle anterior to the epiphyseal bar, and

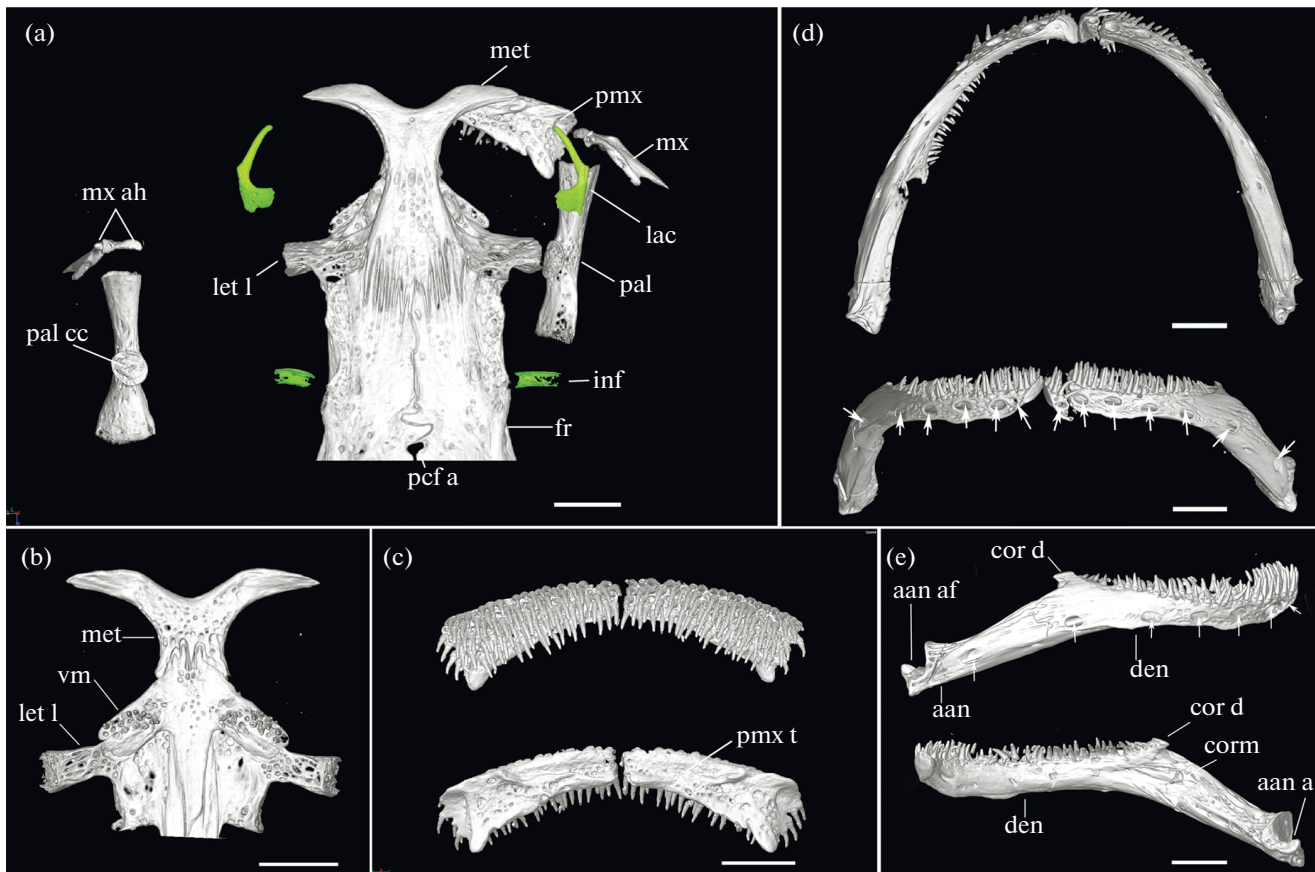


Fig. 4. Snout and jaws of *Proliobagrus dorsalis*, holotype, GIFT 2011050901: (a) snout in dorsal view with left autopalatine and maxilla rotated 90° to expose the medial side, (b) anterior end of neurocranium in ventral view showing vomer, (c) paired premaxilla in ventral and dorsal views, (d) low jaw in ventral and anterior views, (e) right dentary and angulo-articular-retroarticular in lateral and medial views.

aan, angulo-articular-retroarticular; aan af, articular face of angulo-articular-retroarticular; cor d, coronoid process of dentary; corm, coronomeckelian bone; den, dentary; fr, frontal; inf, infraorbital; lac, lacrimal; let l, lateral process of lateral ethmoid; met, mesethmoid; mx, maxilla; mx ah, articular heads of maxilla; pal, autopalatine; pal cc, central condyle of autopalatine; pcf a, anterior remnant of posterior cranial fontanelle; pmx, premaxilla; pmx t, trench in premaxilla; vm, vomer; (→) opening of sensory canal running through dentary. Scale: 1.0 mm.

again meet medially posterior to the epiphyseal bar but leaving aperture-like anterior remnant of posterior cranial fontanelle (Figs. 3a, 4a). The posterior subdivision of the posterior cranial fontanelle extends widely into the supraoccipital, nearly to its occipital margin, and anteriorly framed by the posteromedial margin of the frontals (Fig. 3a). The frontal has a relatively straight orbital (lateral) margin, dorsally obscuring the orbitosphenoid and pterosphenoid in side walls of skull. The sphenotic is similar in size to the pterotic. The sphenotic articulates medially with the postero-lateral margin of the frontal, posteriorly with the anterolateral margin of the supraoccipital and a short anterior margin of the pterotic. The sphenotic has a flat, pointed sphenotic process, projecting horizontally off the skull roof margin, instead of an anterolateral process extending forward. The lateral margin of the sphenotic forms a narrowly elongated articular fossa for the articular head of hyomandibula (Fig. 3b),

and the hyomandibula articulation is limited the lateral margin of the sphenotic. The pterotic is postero-laterally expanded and rounded. The pterotic sutures medially with the supraoccipital, anteriorly with the sphenotic, and posteriorly with the epioccipital. The supraoccipital is large, deeply notched medially with a tiny posterior process, and the transverse crests is sharply well-defined and along the occipital margin.

The occipital wall of the skull is formed by the supraoccipital, exoccipitals, epioccipitals, and basioccipital (Figs. 3c, 3d). The exoccipital is relatively large, forming the posteroventral corner of the neurocranium. The foramen magnum is framed dorsally by supraoccipital, laterally and ventrally by exoccipitals. Ventromedially belowing the foramen magnum, a bony canal forms sinus impar for passage of medial extension of inner ear toward Weberian ossicles. The foramina for glossopharyngeal and vagus nerves are located near the posteroventral corner of

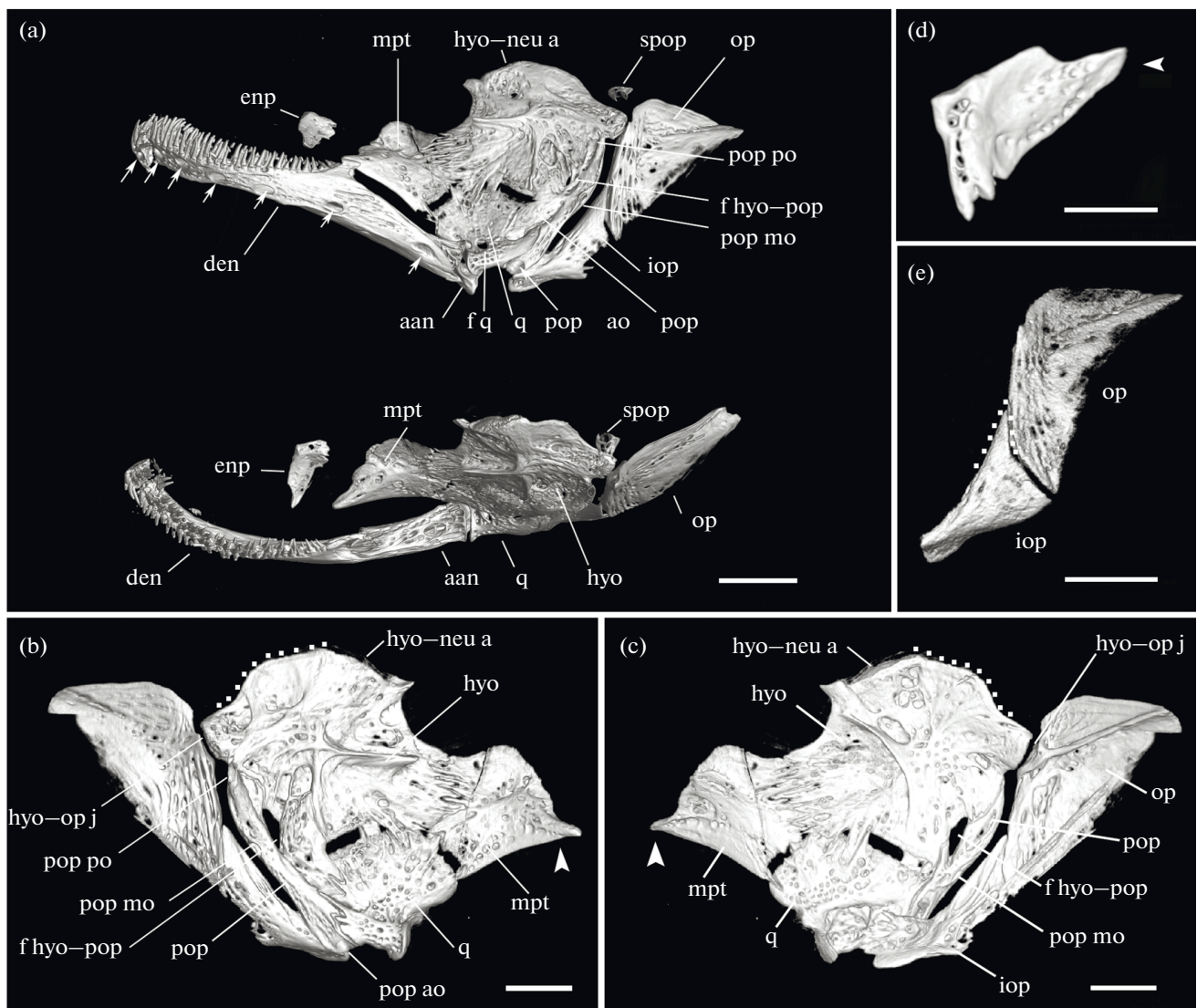


Fig. 5. Suspensorium and opercular bones of *Proliobagrus dorsalis*, holotype, GIF 2011050901: (a) suspensorium with low jaw (left side) in lateral and dorsal views, (b, c) right suspensorium in lateral and medial views, (d) right endopterygoid in dorsal view, rostral end to up, (e) left opercle and interopercle in lateral view.

aan, angulo-articular-retroarticular; den, dentary; enp, endopterygoid; f hyo-pop, foramen between hyomandibula and preopercle; f q, foramen piercing quadrate; hyo, hyomandibula; hyo-neu a, articular facet of hyomandibula for neurocranium; hyo-op j, hyomandibula-opercle joint; iop, interopercle; mpt, metapterygoid; op, opercle; pop, preopercle; pop ao, mo, po, anterior, medial, posterior opening of sensory canal on preopercle; q, quadrate; spop, superapreopercle. (→) opening of sensory canal running dentary in (a); (...) the margin of posterodorsal expansion of the hyomandibula in (b, c), and the margin of posterodorsal intension of interopercle in (e); (◀) anterolateral process of the endopterygoid in (d), and condylar anterior process of metapterygoid in (b, c). Scale, mm: (a, e) 1.5, (b, c) 1.0, (d) 0.6.

the exoccipital. A concave facet develops at the dorsal surface of the epioccipital to accommodate the pterotic (upper) arm of supracleithrum (= “anteromedial process of horizontal lamina of supracleithrum” of Chen, 1994), contacting the posterior margin of the pterotic, and evident in dorsal view. The median basioccipital is the posteriormost element of the neurocranial floor. It posteriorly joints with a separate first vertebra centrum and deeply sutures with the posterior end of the parasphenoid anteriorly.

The large elongate parasphenoid forms the major part of neurocranial floor from the mesethmoid and vomer to the basioccipital. The parasphenoid has wing-like expansions adjacent to the orbitosphenoid, pterosphenoids and prootics. The prootic is large, posterior to the lateral wing of the parasphenoid, contacting the basioccipital and exoccipital posteriorly, sphenotic and pterotic dorsolaterally, which together form the otic capsule. There is a shallow fossa among the prootic, exoccipital, and the pterotic. The orbito-

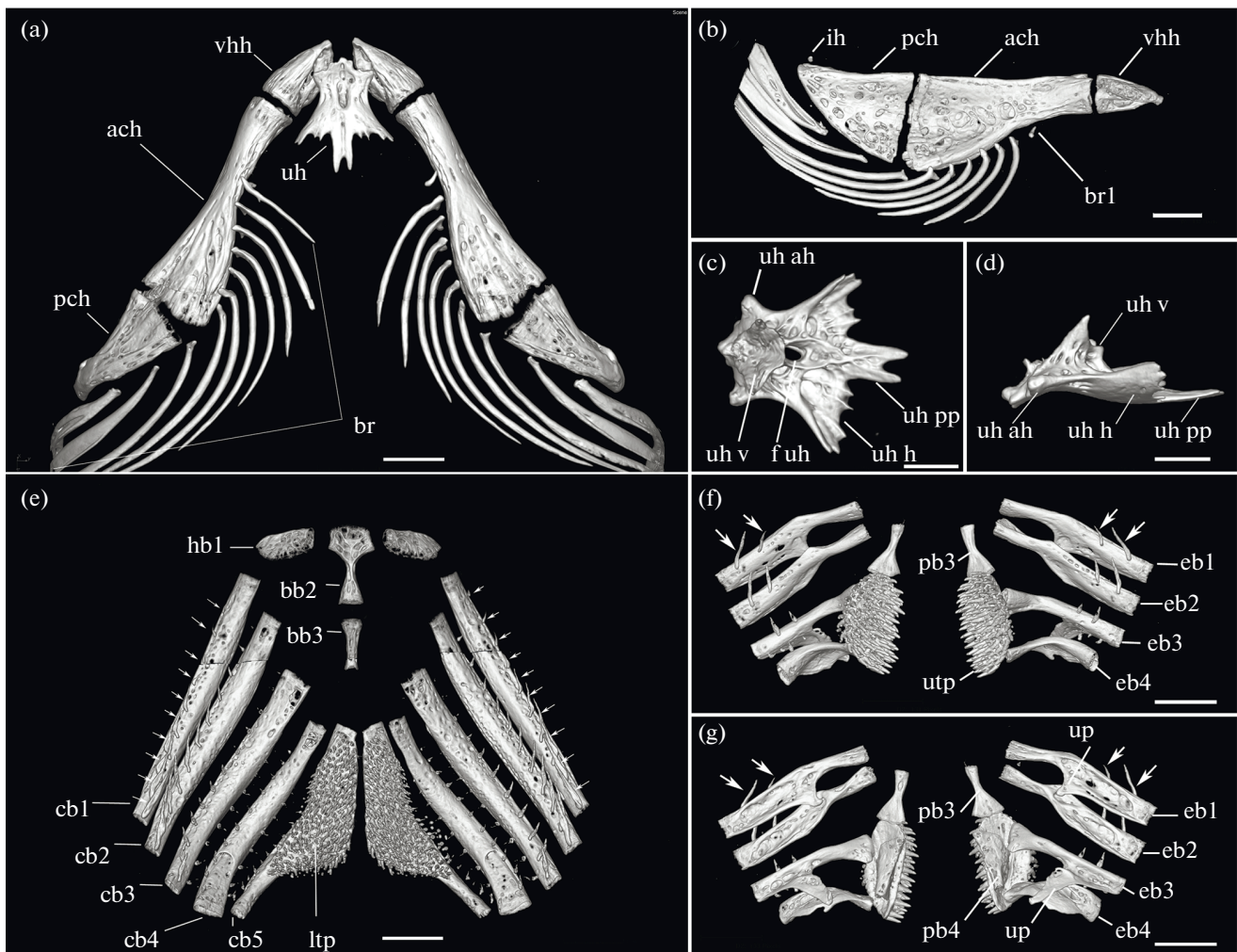


Fig. 6. Hyoid and branchial arches of *Proliobagrus dorsalis*, holotype, GIF 2011050901: (a) hyoid arch in ventral view, anterior to up, (b) left hyoid bar (the hypohyal, anterior and posterior ceratohyals, and interhyal) in medial view, (c, d) urohyal in dorsal and lateral views, (e) ventral elements of branchial arch in dorsal view, and dorsal elements of brachial arch in ventral (f) and dorsal (g) view.

ach, anterior ceratohyal; bb2, 3, basibranchial 2, 3; br, branchiostegal rays; cb 1-5, ceratobranchial 1-5; eb 1-4, epibranchial 1-4; f uh, foramen piercing urohyal; hb1, hypobranchial 1; ih, interhyal; ltp, lower tooth plate; pb3, 4, pharyngobranchial 3, 4; pch, posterior ceratohyal; uh, urohyal; uh ah, articular head of urohyal; uh pp, posterior process of urohyal; uh h, horizontal lamina of urohyal; uh v, vertical lamina of urohyal; utp, upper tooth plate; up, uncinate process; vhh, ventral hypohyal. (→) gill rakers on ceratobranchial 1 in (e); (→) gill rakers on epibranchial 1 in (f, g). Scale, mm: (a, b, e-g) 1.0, (c, d) 0.5.

sphenoid is anterior to its lateral wing, contacting the anterior span of the parasphenoid ventromedially. A small opening possible for an artery is present between posteroventral corner of the orbitosphenoid and anterior base of the parasphenoid wing ("f in" in Fig. 3c). The vomer is arrow-head shaped, suturing with mesethmoid anteriorly, and with the anterior end of parasphenoid ventrally via its short posterior process (Fig. 3b). The lateral processes of the vomer barely reach the base of antorbital process of the lateral ethmoid (Figs. 3b, 4b), laterally bearing two patches of teeth widely separated across midline.

The exit foramina for the facial, trigeminal (and optic) nerves sit on the orbit wall of neurocranium

from the posterior to the anterior (Fig. 3c). A small posterior foramen likely that of a facial nerve branch, is bounded dorsally by the sphenotic and ventrally by the prootic. A large foramen for trigeminal and possibly branches of facial nerve is framed by the bony septum of the sphenotic posterodorsally, the pterosphenoid anterodorsally, and the parasphenoid wing ventrally. Possible optic nerve foramen is reduced in size between the orbitosphenoid and pterosphenoid. A small anteriorly directed foramen traverses anterior portion of the pterosphenoid with undetermined function ("f inpt" in Fig. 3f).

The infraorbital series is reduced to two elements (Fig. 4a): the lacrimal (the first infraorbital bone) and

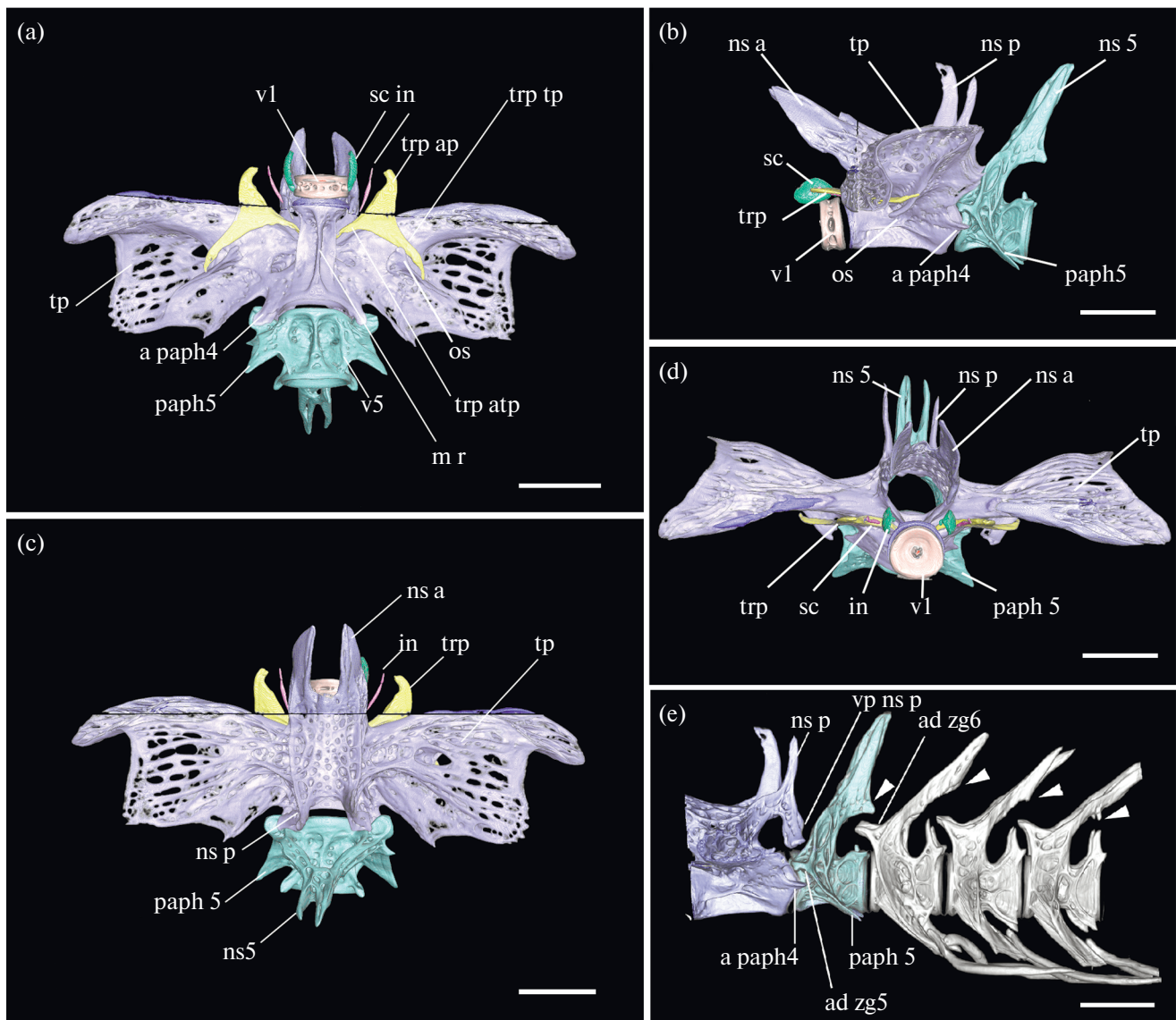


Fig. 7. Weberian apparatus plus vertebra 5 of *Proliobagrus dorsalis*, holotype, GIF 2011050901: (a) ventral view, (b) lateral view with rostral end to left, (c) dorsal view, (d) anterior view, (e) posterior Weberian apparatus plus anterior vertebrae 5–8 in lateral view with left transvers lamina removed, rostral end to left.

ad zg 5, 6, anterodorsal zygapophysis of vertebra 5, 6; a paph4, auxillary parapophysis of compound Weberian centrum; in, intercalarium; m r, median ridge; ns a, anterior neural spine of the compound Weberian centrum; ns p, posterior neural spine of compound Weberian centrum; ns 5, neural spine of vertebra 5; os, ossified suspensorium; paph5, parapophysis of vertebra 5; sc, scaphium; tp, transverse process of the compound Weberian centrum; trp ap, atp, tp, anterior process, articular process, transformator process of tripus; v1,5, vertebra 1, 5; vp ns p, ventral process of posterior neural spine of the compound Weberian centrum; (◀) the tiny ventral process of neural spine of vertebra 5–7 in (e). Scale: 1.0 mm.

the posteriormost infraorbital. The lacrimal is plate-like, bearing no canal, and itapering anteriorly to premaxilla and posteriorly expanded with a dorsal process. The posteriormost infraorbital is tubular, perpendicular to the midline.

A simple, wide sensory canal, comprised of the postotic, otic, and supraorbital canals, runs through the lateral margin of the skull roof and is continuous anteriorly with that in the nasal. The exit of the preopercular canal is on the pterotic, and the exit of infra-

orbital canal is on the frontal at the vertical of the epiphyseal bar, thus the otic canal is relative long and runs through the pterotic, sphenoic, and frontal. Except two short branches connecting the preopercular and infraorbital canals, there is lack any other branches such as the epiphyseal branch, parietal branch. One wide opening sits dorsally on the mid-point of the frontal segment of the supraorbital canal.

Jaws and autopatine (Fig. 4). The upper jaws comprise the premaxilla and maxilla. The premaxilla

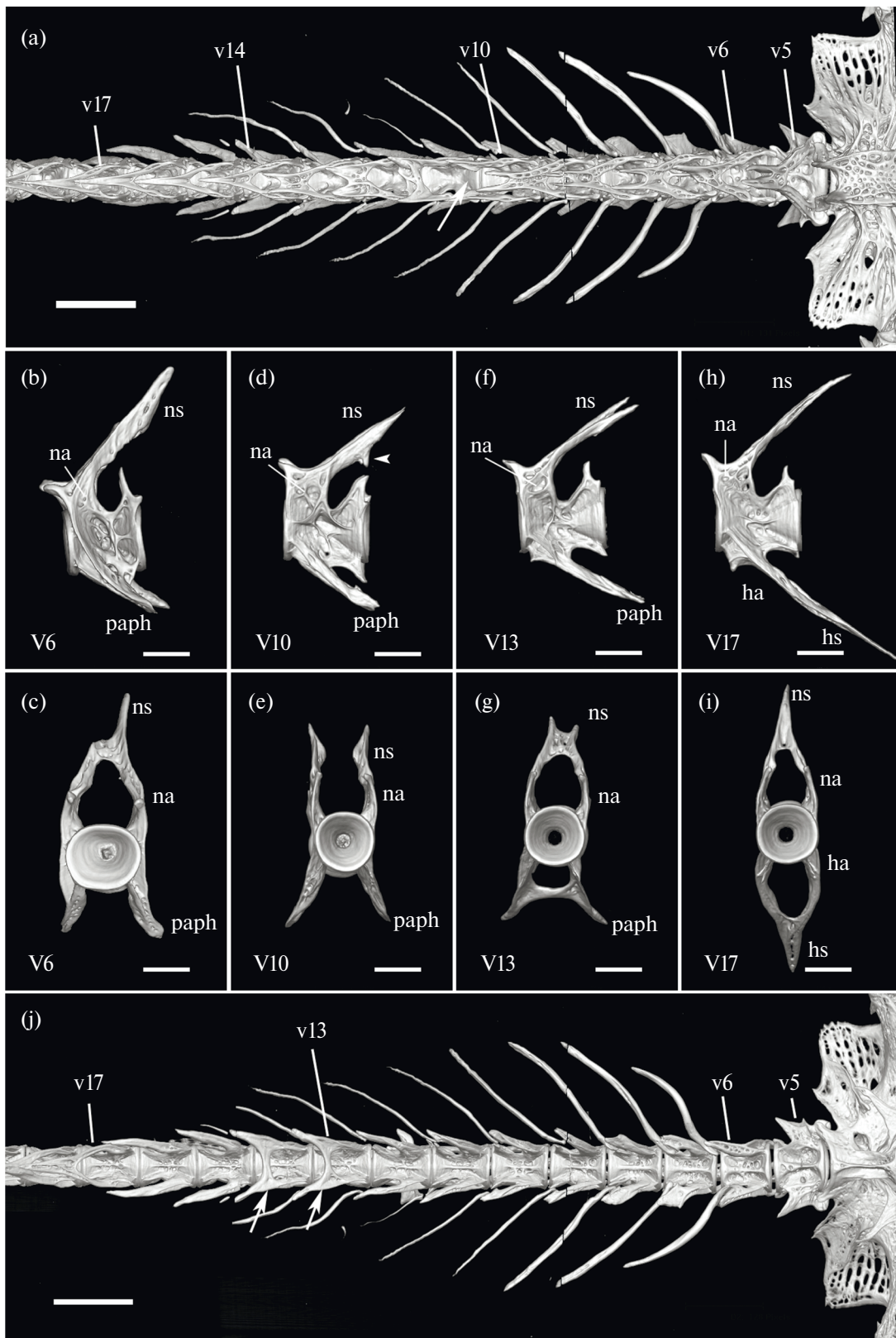


Fig. 8. Vertebrae of *Proliobagrus dorsalis*, holotype, GIFT 2011050901: (a) precaudal vertebrae in dorsal view, rostral end to right; (b, d, f, h) representative vertebra in lateral view, (c, e, g, i) representative vertebra in anterior view, (j) precaudal vertebrae in ventral view, rostral end to right. (b, c) vertebra 6, (d, e) vertebra 10, (f, G) vertebra 13, (h, i) vertebra 17.

ha, haemal arch; hs, haemal spine; na, neural arch; ns, neural spine; paph, parapophysis; v5, 6, 10, 13, 14, 17, vertebra 5, 6, 10, 13, 14, 17. (◀) ventral process of neural spine in (d); (→) ventral arch in (j). Scale: (a, j) 1.5, (b-i) 0.6 mm.

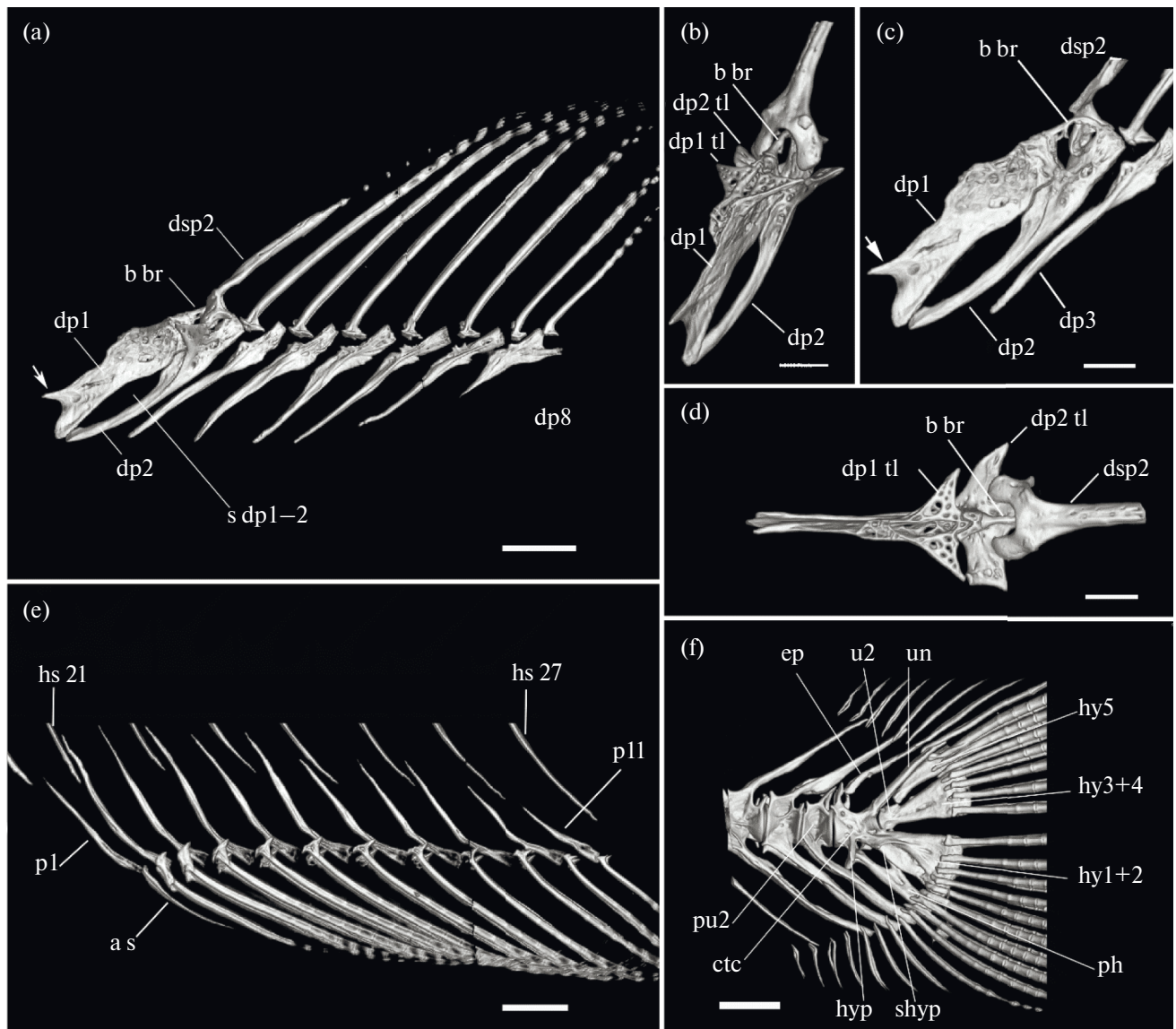


Fig. 9. Median fins and supports of *Proliobagrus dorsalis*, holotype, GIFT 2011050901: (a) dorsal fin skeleton, (b–d) first and second dorsal-fin pterygiophores and associated elements in oblique-, cutaway-, dorsal views (left transverse lamina of first and second dorsal-fin pterygiophores, and left hemitrich of dorsal spine 2 removed in (c)), (e) anal fin skeleton, (f) caudal skeleton. Rosstral end to left in all panels, (→) anteriorly directed process in (a, c).

a s, spine of anal fin; b br, bony bridge; ctc, compound terminal centrum; dp 1, 2, 3, 8, dorsal-fin pterygiophore 1, 2, 3, 8; dp1 tl, transverse lamina of first dorsal-fin pterygiophore; dp2 tl, transverse lamina of second dorsal-fin pterygiophore; dsp 2, second dorsal spine; ep, epural; hs 21, 27, haemal spine of vertebra 21, 27; hy 1–4, fused hypural 1 and 2, 3 and 4 respectively; hy 5, hypural 5; hyp, hypurapophysis; p1, 11, pterygiophore 1, 11; ph, parhypural; pu 2, preural 2; s dp1–2, space between first and second dorsal-fin pterygiophore; shyp, secondary hypurapophysis; u 2, ural 2; un, uroneural. Scale: (a, e, f) 1.0, (b–d) 0.5 mm.

is subrectangular, narrow longitudinally, about 3.75 times wider than long (Fig. 4c). It dorsally articulates with the mesethmoid cornua through a shallow trench on its dorsal surface (Figs. 4a, 4c). The ventral surface of the premaxilla is covered with four to five rows of narrowly conical, tall teeth except a short edentulous posterolateral process (Fig. 4c). The maxilla is edentulous, setting off laterally from the premaxilla. The maxillary shaft is shallowly grooved post-axially wherein lies the elastocartilage core of the maxillary

barbell. Its distal margin is notched (Fig. 4a). The maxillary head is bifid with a dorsoventral pair of condyles that articulates with the anterior cartilage of the autopalatine.

The autopalatine, longitudinally oriented lateral to the lateral ethmoid, is stout and rod-like with both ends cartilage-capped (Fig. 4a). The autopalatine has a circular mediocentral condyle through which articulates with the cartilage of antorbital process of the lat-

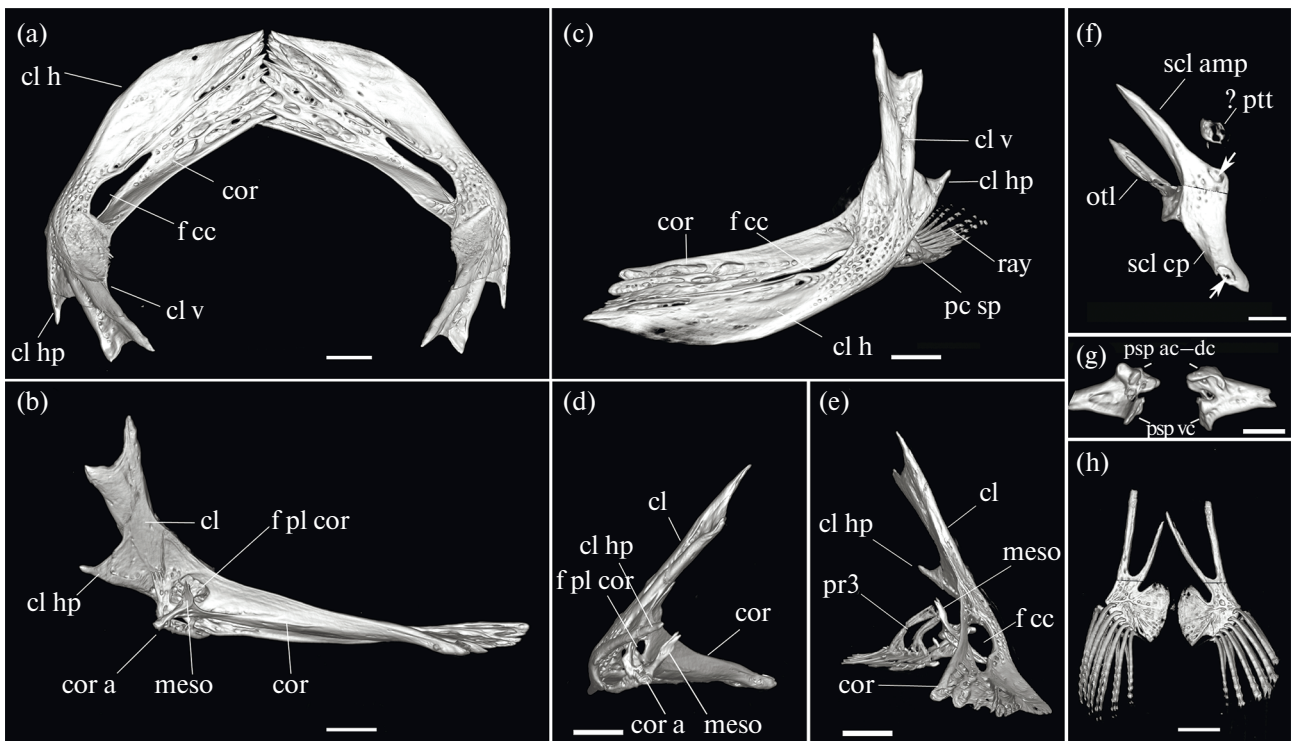


Fig. 10. Pectoral and pelvic girdles of *Proliobagrus dorsalis*, holotype, GIF 2011050901: (a) paired pectoral girdles in dorsal view, (b) left pectoral girdle in medial-oblique view, (c) left pectoral girdle with pectoral-fin rays in latero-oblique view, (d) left pectoral girdle in posterior view, (e) left pectoral girdle in antero-oblique view, (f) right supracleithrum in dorsal view, (g) left pectoral spine head in medial (left one) and lateral (right one) views, (h) pelvic girdle and fins in ventral view.

cl, cleithrum; cl h, horizontal limb of cleithrum; cl hp, humeral process of cleithrum; cl v, vertical limb of cleithrum; cor, coracoid; cor a, articular condyle of coracoid for complex radial; f cc, foramen between cleithrum and coracoid; f pl cor, posterolateral foramen of coracoid; meso, mesocoracoid; otl, ossified transcapular ligament; pc sp, pectoral spine; psp ac-dc, anterior-dorsal articular head of pectoral spine; psp vc, ventral articular head of pectoral spine; pr3, proximal radial 3; ptt, posttemporal; scl amp, anteromedial process of supracleithrum; scl cp, cleithral process of supracleithrum. (→) opening of sensory canal in (f). Scale, mm (a–e, h) 1.0, (f, g) 0.5.

eral ethmoid. The posterior part of the autopalatine (posterior to the medilcentral condyle) is laterally compressed and dorsoventrally expanded.

The lower jaw comprises the dentary, the fused-articular-retroarticular complex, and coronomeckelian bone (Meckelian ossicle). The dentaries meet in a loose symphysis with direct bony contact limited to dorsal edge (Fig. 4d). The dentary is narrow and shallow throughout (Figs. 4d, 4e), and the coronoid process of the mandible comprises only the dorsal edge of the dentary, without angular component (Fig. 4e). The dentary bears one to three rows of teeth in a posteriorly narrowing band extending from the symphysis onto the coronoid process. The medial trench ventral to the coronoid process accommodates the Meckel's cartilage and a tiny coronomeckelian bone (Fig. 4e). The articular fossa of the jaw joint is deep with a posterior process off the angulo-articular-retroarticular (Fig. 4e).

The mandibular sensory canal runs through the dentary (Figs. 4d, 4e), and bears seven large oval-

shaped foramina, with the anterior five equally spaced, the sixth foramen below the coronoid process, and the seventh foramen adjacent to articular fossa of the angulo-articular-retroarticular. The mandibular sensory canal does not enter the angulo-articular-retroarticular, and the preoperculo-mandibular sensory canal is disconnected.

Suspensorium and opercular bones (Fig. 5). The suspensorium comprises the endopterygoid (= entopterygoid in Arratia), metapterygoid, quadrate, hyomandibula, and preopercle. The endopterygoid is ventral to the posterior limb of the autopalatine, ligamentously connected to the metapterygoid (Fig. 5a). It is roughly rectangular, with a prominently notch at its anterolateral corner to form a pointed lateral process (Fig. 5d). The metapterygoid is roughly pentagonal with an anterior process, and posteriorly interdigitates with the hyomandibula (Figs. 5b, 5c). The quadrate is fan-like dorsal to its anteroventral articular condyle, and lacks conspicuous anterior extension (Figs. 5b, 5c). It articulates with the metapterygoid, hyomandibula, and preopercle. The

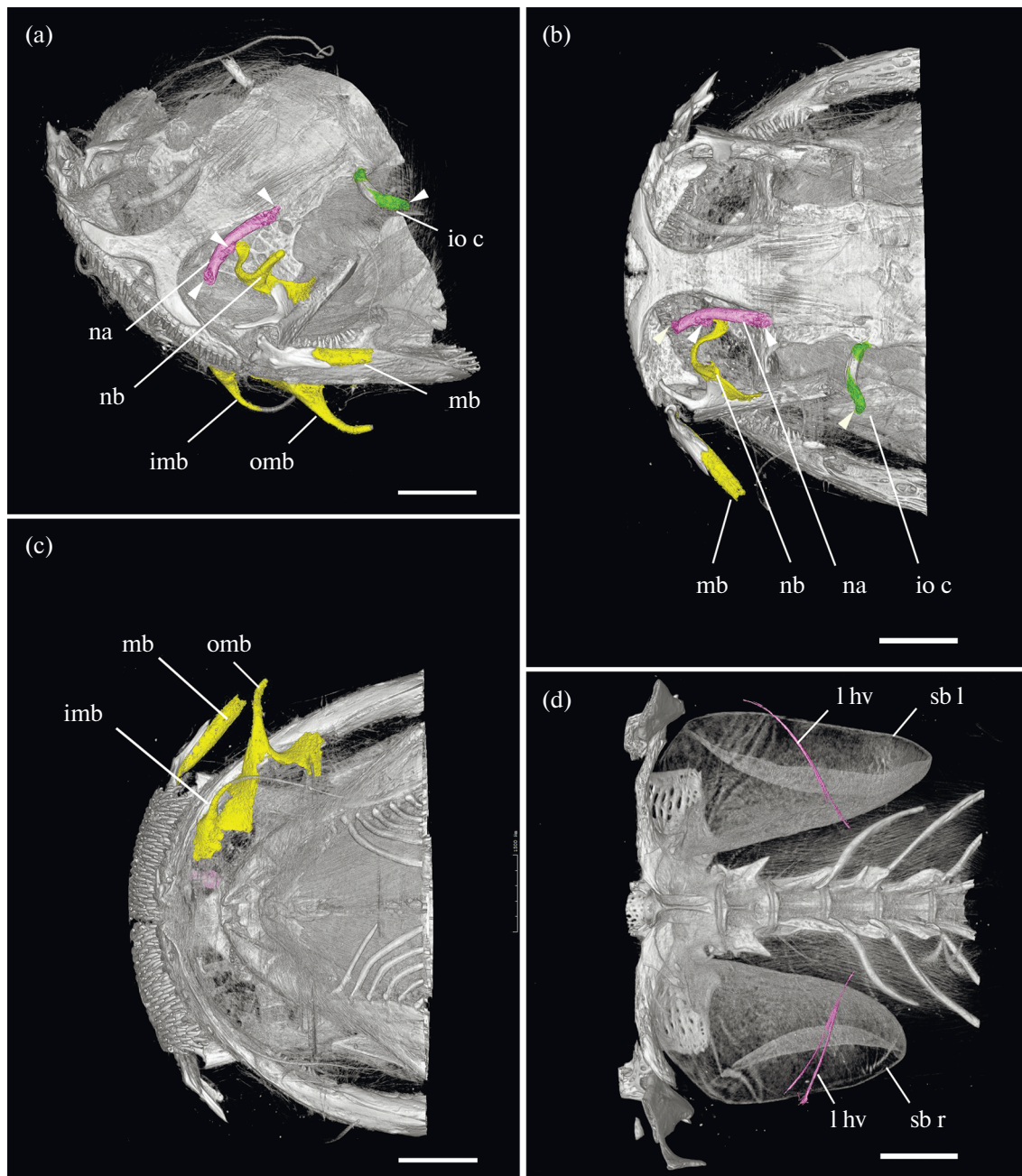


Fig. 11. Features of unossified tissues of *Proliobagrus dorsalis*, holotype, GIFT 2011050901: (a–c) snout region with basal part of the barbels and their supports, nasal and infraorbital canals in oblique-anterior, dorsal, and ventral views; (d) humerovertebral ligament and swimbladder in ventral view; the lateral wall of swimbladder sac was depressed.

io c, infraorbital canal; na, nasal; nb, basal part of nasal barbel; mb, basal part of maxillary barbel; imb, basal part of inner mental barbel; omb, basal part of outer mental barbel; l hv, humerovertebral ligament; sb l, left lobe of swimbladder; sb r, right lobe of swimbladder. (◀) pores of nasal canal and infraorbital canal. Scale: 1.5 mm.

quadrate-metapterygoid joint is bony and sutural at its ventral and dorsal ends, centrally synchondral with persistent pterygo-quadratus cartilage (radiotransparent). The quadratus-hyomandibula joint is bony and sutural anteriorly and posteriorly, centrally synchondral with persistent symplectic cartilage (radiotransparent).

The hyomandibula is large, and its posterodorsal corner is expanded, fan shaped, with nearly semi-circular dorsal margin (Figs. 5b, 5c). The hyomandibula articulates with the neurocranium dorsally along the sphenotic via an elongated articulating facet, suturally interdigitating with the metapterygoid anteriorly and the quadratus anteroventrally (Figs. 5b, 5c). It is also

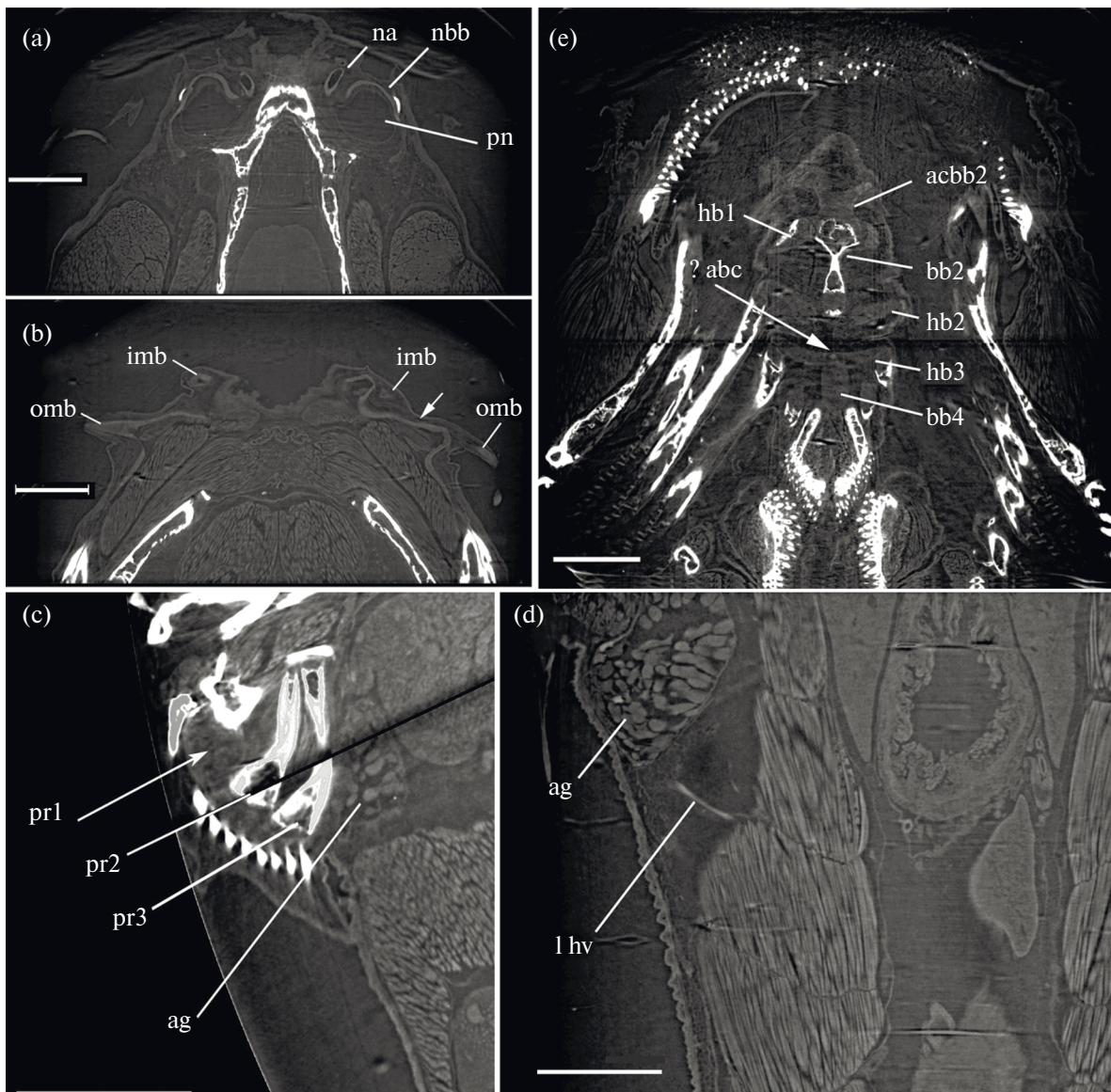


Fig. 12. Virtual sections showing barbel base, proximal pectoral radial 1, humerovertebral ligament, and cartilaginous elements of branchial arch of *Proliobagrus dorsalis*, holotype, GIF 2011050901: (a) virtual slice showing nasal barbel base, (b) “head-to-tail” patterned fusion of base of mental barbel limbs, (→) the fusion of cartilaginous base of inner and outer mental barbels; (c) virtual slice showing auxillary glad and cartilaginous pectoral proximal radial 1, (d) virtual slice showing auxillary glad and a segment of humerovertebral ligament, (e) virtual slice showing cartilaginous elements of branchial arch, (→) putative accessory basibranchial cartilage.

abc, accessory basibranchial cartilage; acbb2, anterior cartilage of basibranchial 2; ag, axillary gland; bb2, 4, basibranchial 2, 4; hb 1–3 hypobranchial 1–3; imb, base of inner mental barbel; 1 hv, humerovertebral ligament; nbb, cartilaginous base of nasal barbel; omb, base of outer mental barbel; pn, posterior nostril; pr1–3, pectoral proximal radial 1–3. Scale: 1.5 mm.

articulates posteriorly with the opercle via a prominent condyle, and posteroventrally tightly covered by trapezoidal bony sheet of the preopercle. A single tubular supra-preopercle is dorsal to the opercular condyle of the hyomandibula (Fig. 5a).

The preopercle is completely incorporated into the suspensorium (Figs. 5a–5c). It is vertically extended with thick, rod-like posterior margin containing sensory canal with anterior, medial, and posterior foramina

(Fig. 5b). The preopercle and hyomandibula enclose a wide mandibularis foramen for the mandibularis ramus of facial nerve (Fig. 5b).

The opercle is roughly triangular, articulating with hyomandibula at its anterodorsal corner (Figs. 5a–5c). The interopercle is deep posteriorly with a short posterodorsal extension along the convex anteroventral margin of the opercle (Fig. 5e).

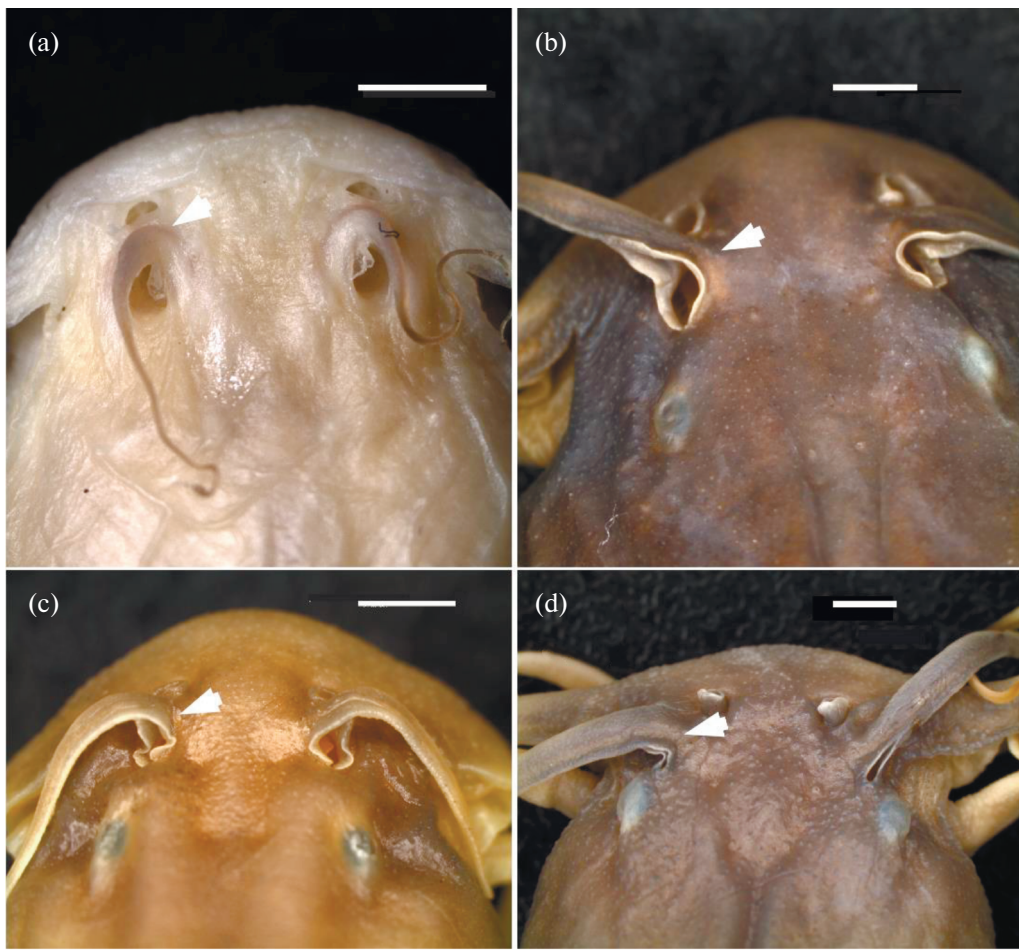


Fig. 13. Snout region with nostrils and base of nasal barbel: (a) *Proliobagrus dorsalis*, holotype, GIF 2011050901; (b) *Xiurenbagrus gigas* LJH 02040108, (c) *X. xiurenensis* LJH 02050849, (d) *Liobagrus* sp. (⇒ base of nasal barbel in (a-d)). Scale: 2 mm.

Hyoid arch and urohyal (Fig. 6). The dorsal hypohyal is absent. The ventral hypohyal caps the hyoid bar, and bears an articular fossa for the urohyal at the lateral anteroventral corner (Fig. 6a). The anterior and posterior ceratohyals are deep and compressed with smoothly rounded and unkeeled dorsal margin. The ventral hypohyal-anterior ceratohyal joint and the anterior ceratohyal-posterior ceratohyal joint are synchondral, lacking direct bony contact (Figs. 6a, 6b). The interhyal is extremely rudimentary (Fig. 6b). There are ten branchiostegal rays on each side (Fig. 6a): seven rays articulating with the anterior ceratohyal, one with the radiotransparent space (cartilaginous) between anterior and posterior ceratohyals, two rays with the posterior ceratohyal. The anteriormost left branchiostegal ray is ossified just at base (Fig. 6b). The postiormost two rays are large and become flattened and wider at their distal ends. The urohyal articulates the paired ventral hypohyals (Fig. 6a). The horizontal lamina of the urohyal bears a median posterior process and paired posterolateral processes, and the vertical lamina of the urohyal is socket shaped, dorsally bifid

from its base (Figs. 6c, 6d). Hypobranchial foramen (Fig. 6c) pierces the urohyal posterior to vertical lamina.

Branchial arches (Fig. 6). There are two ossified basibranchial elements, identified as basibranchials 2 and 3 (Fig. 6e). The basibranchial 2 is spade shaped with an expanded anterior end, and the basibranchial 3 is rod-like. There is one pair of ossified hypobranchial, identified as the hypobranchial 1, medially perpendicular to the lateral margin of basibranchial 2 (Fig. 6e). The hypobranchials 2 and 3 are unossified. Five paired ceratobranchials are ossified (Fig. 6e). Ten gill rakers are present on the anterior margin of the ceratobranchial 1 (Fig. 6e), and ten rakers on the anterior margin of ceratobranchial 2 with increasing length posteriorly. The small gill rakers are also present on both the anterior and posterior margins of the ceratobranchials 3 and 4. The ceratobranchial 5 is stout and carries the pharyngeal tooth plate (Fig. 6e), its anterior two third is triangular and medially expanded. The medial margins of the paired tooth plates nearly meet along the midline. Tiny gill rakers are discernable on the anterior margin of the ceratobranchial 5.

The four paired epibranchials are well ossified. The medial tips of the epibranchials 1 and 2 approach to each other (Figs. 6f, 6g). The epibranchial 1 has an uncinate process off the posterior margin, overlapping the anterior margin of epibranchial 2 (Fig. 6g). The medial tips of epibranchials 3 and 4 are dorsal to the upper pharyngeal tooth plate. The epibranchial 3 has a large, elongate uncinate process off the posterior margin, overlapping the epibranchial 4 (Fig. 6g). The pharyngobranchial 3 is rod-like with an expanded posterior end, and the pharyngobranchial 4 is roughly quadrangular, bearing upper pharyngeal tooth plate (Fig. 6f).

Two gill rakers are present on the anterior margins of the epibranchials 1 and 2 (Fig. 6f), thus twelve gill rakers are present on the first gill arch (ten on the ceratobranchial 1 and two on the epibranchial 1).

Weberian apparatus (Fig. 7). The Weberian apparatus comprises four anteriormost vertebrae as: Weberian complex (pars sustentaculum) and Weberian ossicles (pars auditum). The first centrum is short, disc-shaped lacking any processes. The vertebrae 2 to 4 are fused as the compound Weberian vertebra (Figs. 7a, 7b). It bears a prominent median ridge on its ventral surface (Fig. 7a) and has paired laterally expanded, dorsally-domed sheet-like transverse process (“fourth transverse process” of Chen, 1994, Fig. 24a). The os suspensorium is a small process inclining forward from the ventral surface of the transverse process (Fig. 7b). An additional, short separate process sets posterolaterally off the compound Weberian centrum (possibly paired novel auxillary parapophyses) (Figs. 7a, 7b). The neural arch of the compound Weberian centrum is saddle-shaped, lacking a median dorsal lamina, between its anterior and posterior neural spines (Figs. 7b, 7c). The anterior neural spine (third neural spines) is divided proximally, inclining forward toward occiput (Fig. 7b). The posterior neural spine (fourth neural spine) is bilaterally bifid, slender, its distal end being curved anteriorly (Fig. 7b); a heavy strut-like process extending ventrally off the base of each half of fourth neural spine, similar in length to the neural spine (Fig. 7e).

There are three pairs of Weberian ossicles (Figs. 7a–7c), and the claustrum is absent. The scaphium is large, ovoid, convex, and lacking an ascending process; it is located above the posteriorly protruding basioccipital-the frist centrum joint, with the length a little longer than that of the first centrum. (Fig. 7b). The intercalarium is an elongated and slender ossicle, lateral to the posterior part of scaphium, hidden medially to the anterior process of tripus in lateral view (Figs. 7a, 7c). The tripus is the largest one of the Weberain ossicle. It is roughly triangular with a deeply concave lateral margin, and has three processes (Fig. 7a): an anterior process stubby with a medially curved anterior hook; a short articular process, tapering to a point; a long transformator process curving

laterally, and antero-lateral to the anterior end of the os suspensum (Fig. 7b).

Post-Weberian vertebral column (Fig. 8). There are a total of 39 vertebrae, with 16 precaudal vertebrae (incl. Weberian vertebrae 1–4) and 23 caudal vertebrae (compound terminal centrum, putative preural 1 + ural centrum 1, counted as single element) (Figs. 2b, 8a, 8j). Both pre- and postzygapophyses develops on the neural arch of vertebra 5–38 (Figs. 2b, 8b, 8d, 8f, 8h).

The neural spines of vertebrae 5–13 are bilaterally bifid (Fig. 8a) with a small or tiny ventral process at the neural spine of vertebrae 5–11 (Figs. 2b, 7e, 8d) which is comparable to the heavy strut-like ventral process of 4th neural spine (Fig. 7e). The neural arch of vertebra 10 is open dorsally, and its widely bifid neural spines accommodate the first dorsal-fin pterygiophore (Figs. 8a, 8e; also refer to Fig. 2b). The neural spines of vertebrae 14–37 are united and subequal in length (Fig. 2b), and the neural spine of vertebra 38 (preural centrum 2) is absent (Fig. 9). Vertebrae 6–14 bear paired ribs, which attach poster-ventrally to the distal tips of parapophyses (Figs. 8a, 8j). The lengths of the ribs are gradually decreasing posterior of the second pair, and the last paire on vertebra 14 being vestigial (Figs. 8a, 8j). Anteriormost bony haemal arch connects paired parapophysis of vertebrae 13 and 14 (Figs. 8g, 8j), and the first complete (fused) haemal spine is on vertebra 17 (Figs. 8j, 2b).

Dorsal fin and supports (Figs. 9a–9d). The dorsal fin is supported by one fin spine (second lepidotrichium), seven soft fin rays, and internally braced by eight pterygiophores (Fig. 9a). It is posteriorly displaced. The supraneural 3 and anterior nuchal plate are absent. The first pterygiophore is remote from the Weberian complex, wedged within the bifid neural spines of vertebra 10 (Fig. 2b). The first pterygiophore is a compressed bony lamina, lacking anterior depression and bony canal for transmitting the erector muscles of the spine (Figs. 9b–9d), and a paired transverse lamina develops its dorsal surface with an equilateral triangular shape (Fig. 9d). Its proximal end is anteriorly fused with “a prominent anterior process” (Figs. 9a–9c), which is suspected of a reduced supraneural. The first pterygiophore supports no fin spine. Its middle radial is not completely fused to the proximal radial (Figs. 9b–d), and extends into the articular foramen of following fin spine to form a bony bridge by fusing with the distal end of the second pterygiophore (Fig. 9c). The second pterygiophore is gently expanded distally, laterally keeled, and tapering anteroventrally. The first two pterygiophores are in contact proximally and distally (Figs. 9a, 9c). A paired laterally expanded wings develop as the dorsal surface of the second pterygiophore (Fig. 9d), broader than the distally expanded transverse lamina of the first pterygiophore. The spine supported by the second pterygiophore is long, and its shaft is ovoid in cross-section and without longitudinal grooves or dentations

(Figs. 9a, 9b, 9d). Following pterygiophores are rod-like proximally, and vertically expanded distally. The pterygiophore 7 is shorter than anterior pterygiophores, and the pterygiophore 8 lacks rod-like proximal portion (Fig. 9a). The distal ends of pterygiophores 3–7 are fused with proximal-middle radials, and posterodorsally extend toward their corresponding fin rays (Fig. 9a).

Anal fin and supports (Fig. 9e). The anal fin is supported by twelve fin rays, and internally braced by eleven pterygiophores. The fin ray is unsegmented and the others are segmented. The first pterygiophore inserts between the haemal spines of vertebrae 20 and 21, and the second pterygiophore is just posterior to the haemal spine of vertebra 21. Insertion pattern of fin pterygiophores into adjacent haemal spines is: 1, 2, 2, 2, 1, 2, 1. The second pterygiophore is longer than the first one and similar to the pterygiophores 3 to 6 in length. The pterygiophores 7 to 9 are similar to the first pterygiophore in length, and the posteriormost two are diminished in size. The paired hemitrich bases of each ray clasp the distal radial of the anterior pterygiophore, which in turn contacts the proximal-middle radial and anterior margin of following pterygiophore except last ray. The second pterygiophore bears first two segmented rays, and the two rays are in a supernumerary position.

Caudal fin and skeleton (Fig. 9f). The caudal fin is emarginate in form (Fig. 2a). There are 16 principal caudal-fin rays ($7 + 9$) with seven in dorsal lobe of caudal fin and nine in ventral lobe, eight dorsal procurent caudal-fin rays with the anteriormost one placing between the neural spines of the preural centra 4 and 5, and eight ventral procurent caudal-fin rays with the anteriormost one between the neural spines of the presural centra 5 and 6.

The caudal skeleton comprises four separate hypural elements: the parhypural, fused hypural 1 and 2, fused hypural 3 and 4, hypural 5 (= Ph; $1 + 2; 3 + 4; 5$ in Lundberg and Baskin, 1969). The parhypural is separated from the hypural 1 + 2. The hypural 1 + 2 is fused with the compound terminal centrum. The second ural centrum is well-formed, ankylosed with the hypural 3+4, and articulating with the compound terminal centrum by an expanded intervertebral joint (referred as the type 3 U2 of de Pinna and Ng, 2004). The hypural 5 is autogenous. A broad hypural diastema separates both series of hypurals. A pair of hyprapophyses is evident at the compound terminal centrum. A single epural is free above the neural arch of the compound terminal centrum and bent upward. The second preural centrum bears a vestigial neural arch dorsally lacking the neural spine.

Pectoral girdle and rays (Fig. 10a–10g). The pectoral girdle comprises cleithrum, coracoid, supracleithrum, and pectoral radials. The vertical limb of cleithrum has a bifurcated dorsal end, and a short, acutely tipped postcleithral (humeral) process

(Figs. 10a–10c); the horizontal limb of the cleithrum meets its antimere on a short midline suture (Fig. 10a). The coracoid contacts lateroposteriorly the medial face of the vertical limb of the cleithrum, and lateroanteriorly the posterior margin of horizontal limb of the cleithrum, and medially meets its antimere on the midline in a long interdigitating suture (Fig. 10a). The posterior margin of the paired coracoids is roughly parallel to the anterior margin of the paired horizontal limbs of the cleithrum. The posterolateral foramen of the coracoid is large (Figs. 10b, 10d). There are two coracoid articular condyles at the posterior end of the coracoid with the lateral one lodging with medial groove of pectoral spine base and the medial one articulating with complex radial (Fig. 10d). Mesocoracoid arch is incomplete. The mesocoracoid does not contact the coracoid dorsally (Figs. 10d, 10e; also refer to 10b), and its ascending process with a prominent bifid tip.

The supracleithrum (Fig. 10f) is three-dimensionally complex, and has three processes as follows. (1) An anteromedial (pterotic) process reaches and loosely articulates with the dorsal articular fossa of the epioccipital (Fig. 2c). (2) An ossified transcapular ligament is shorter than anteromedial process, and does not contact the basicranium. (3) A cleithral process bearing laterosensory canal medially contact the dorsal end of the vertical limb of the cleithrum (refer to Fig. 2c). A tubular ossicle bearing laterosensory canal (Fig. 10f) is present between the anterior end of cleithral process and the pterotic (Fig. 2b), which is interpreted as a putative posttemporal following Kubicek (2022).

The pectoral spine is short and lacks the longitudinal groove along its anterior edge and serrations along its posterior edge. Pectoral-spine base complex has three articulating condyles (Fig. 10g). The anterior condyle is not prominent and partially fused with the dorsal condyle. Proximal pectoral radial 1 is a roughly round cartilage (Fig. 12c). Proximal pectoral radials 2 and 3 are ossified, elongate, gently expanding posteriorly (Fig. 10e). Eight pectoral-fin rays follow the pectoral spine.

Basipterygium (Fig. 10h). The basipterygium bears two slender anterior processes. Both internal and external anterior processes are straight and similar in width. The internal process is close to the antimere at the anterior end. It lacks any shelf or ridge on its ventral surface. Six pelvic-fin rays articulate with basipterygial posterior margin.

Several characters of unossified tissues (Figs. 11, 12). The unossified tissues, including cartilaginous and ligamentous elements, are discernable in the virtual sections, and several characters are reconstructed and described in the following.

Nasal canal and infraorbital canal (Figs. 11a, 11b). The supraorbital sensory canal passes from the frontal through the nasal. Nasal tubular is weakly ossified, lying along mesethmoid neck, and bears three foram-

ina connecting individual sensory canal pores (Fig. 11a). The infraorbital canal sets off the supraorbital canal from the frontal and passing through a tubular bony infraorbital, then transforms to a short unossified canal with terminating at a pore (Figs. 11a, 11b), instead of extending anteriorly.

Barbel-supporting cartilages (Figs. 11a–11c, 12a, 12b). Cartilaginous base of nasal barbel sits along anterior rim of posterior nostril (Figs. 11a, 11b, 12a). Cartilaginous base is associated with lateral (outer) and medial (inner) mental barbels in a “head-to-tail” connection pattern (Chen, 1994) with tail of posterior limb of inner mental barbel continuous with head of anterior limb of outer mental barbel of same side (Figs. 11c, 12b). Cartilaginous base of maxillary barbel dorsolaterally attaches to the maxilla (Figs. 11a–11c).

Humerovertebral ligament is posterodorsally attached to the base of rib on vertebra 6 and anteroventrally ends in putative muscle tissue associated with axillary gland (Figs. 11d, 12d). First proximal pectoral radial is roughly round, evident in virtual sections (Fig. 12c).

Cartilage of branchial arches (Fig. 12e). Ossified basibranchial 2 is spade shaped, with an anterior cartilage. Cartilaginous basibranchial 4 is apparently not as broad as that in amblycipitids (Chen, 1994, Figs. 54–56; Sun, 2011, Figs. 4, 5). Hypobranchials 2 and 3 are unossified and slender. A radio-dense dot among paired hypobranchial 3 and basibranchial 4 is discernable, which is tentatively interpreted as accessory branchial cartilage.

External morphology (Figs. 1a, 2, 13). Posterior nostrils lack flap, and the base of nasal barbel is along the anterior margin of posterior nostril, separated from the anterior nostril (Fig. 13a). Skin is smooth with lack of any tubercle (Figs. 1a, 2a). Adipose fin confluent with caudal fin (Figs. 1a, 2a). Pseudotympanum is unusually wide, exposing swimbladder externally visible (Figs. 1a, 2a).

DISCUSSION

In this study, we describe and illustrate in detail the skeleton of the holotype of *P. dorsalis*. Based on the observed features, comparative specimens, and related literature, we review the characteristics of *P. dorsalis* in the Sisoroidea, and assess its systematic position by osteological comparisons. A first cladistic analysis is performed. The phylogenetic framework follows a recent phylogenetic arrangement of Siluriformes (Lundberg et al., 2014) in which the Sisoroidea is a member of the Big Asian clade of Sullivan et al. (2006). The synapomorphies diagnosing Amblycipitidae proposed by Chen (1994) are also reviewed.

Comparison with the Superfamily Sisoroidea

De Pinna (1996) provided seven diagnostic characters in support of his Sisoroidea including Akysidae, Amblycipitidae, Aspredinidae, Eretistidae (now a subgroup of Sisoridae) and Sisoridae, then de Pinna and Ng (2004) added one additional character related to caudal skeleton and suggested three out of the previous seven as “homoplasy-free synapomorphies”. Thus, they proposed the diagnostic characters as the following: (1) the compressed and vertically expanded posterior end of the autopalatine; (2) the articular region of the lateral ethmoid laterally elongated by its articular facet for the autopalatine; (3) the presence of a humerovertebral ligament connecting the humeral process of cleithrum — or adjacent soft tissue — to anterior portion of fifth or sixth vertebra; 4—the presence of a well-formed second ural centrum (de Pinna and Ng, 2004). As pointed out by de Pinna (1996), the configuration of humerovertebral ligament varies in the attachment sites. In the Akysidae, this ligament attaches anteriorly on the humeral process of the cleithrum and posteriorly on the sixth parapophysis. In the Amblycipitidae, it attaches anteriorly on the soft tissue of the axillary gland and posteriorly on the sixth parapophysis or the sixth rib in examined specimens of *Amblyceps mangois*, *Liebagrus anguillicauda*, *Liebagrus reini* (de Pinna, 1996). In the Sisoridae and south American Aspredinidae, it attaches anteriorly on the humeral process of the cleithrum and posteriorly on the fifth parapophysis, but this condition is considered convergent for these two families (Ng, 2015) as the attachment sites on the fifth parapophysis differ (Ng, 2010, Fig. 11). It should be noted that this ligament is absent in glyptosternines (Ng, 2015) and in *Parakysis* (de Pinna, 1996).

Given the uncertainty in the homology of the humerovertebral ligament, it is not a valid diagnostic character for a monophyletic clade. Instead, we identify the presence of a transverse bilobed swimbladder as another diagnostic character for the Sisoroidea. Thus, we recognize that four characters (three in the above account 1, 2, 4 proposed by de Pinna and Ng (2004) and the bilobed swimbladder) can be used to diagnose the Asian superfamily Sisoroidea (sensu Sullivan et al., 2008). As *Proliobagrus dorsalis* possesses these four diagnostic characters (Figs. 4a, 9f; also Figs. 2b, 3a, 3b), this species is assigned to the superfamily Sisoroidea, but familial assignment was not straightforward at the first glance.

Proliobagrus dorsalis can be excluded from both the Akysidae and Sisoridae due to the absence of synapomorphies that diagnose either family: for the Akysidae (Chen, 1994; de Pinna, 1996) and for the Sisoridae (Ng, 2010, 2015). *Proliobagrus dorsalis* is further distinguished from akysids by morphological differences, such as the absence of tubercles on the skin (vs. presence of tubercles on the skin in the Akysidae), uniform body depth from head to caudal-fin base (vs. body

depth decreasing posterior of dorsal fin base in the Akysidae except in *Parakysis*), and separation of the supracleithrum from the skull roof (vs. an ankylosis between this bone and the skull roof).

As for comparison with the Amblycipitidae, *Proliobagrus dorsalis* is externally diagnosed by the posteriorly displaced dorsal fin, long nasal barbel and its distinct base, and presence of pseudotympanum, which, on top of translucent body and absence of eyes, readily distinguish this species from known amblycipitid genera. Chen and Lundberg (1995) identified three genera, *Amblyceps*, *Liobagrus*, *Xiurenbagrus* within the Amblycipitidae, and proposed the diagnostic characters for each of them. *Proliobagrus* lacks the synapomorphies of *Amblyceps*: (1) the presence of epiphyseal commissure of supraorbital canal; (2) the posterior end of fifth ceratobranchial expanding medially; (3) the presence of pinnate-like rays in procurent caudal fin rays; (4) triangular fenestrae in mental barbel-supporting cartilages immediately medial to both outer and inner mental barbels. *Proliobagrus* is similar to *Xiurenbagrus* in the presence of vomerine teeth (Fig. 4b), lack of deep grooves along shafts of dorsal- and pectoral-fin spines (Fig. 9d), absence of subpterotic process of supracleithrum (Fig. 10f), whereas it is similar to *Liobagrus* in the absence of parietal branch of supraorbital canal (Fig. 3a), adipose fin confluent with caudal fin (Fig. 2a), relative broad snout (Fig. 13a). Furthermore, our osteological study reveals a set of features setting *P. dorsalis* apart from all other sisoroid genera. We review the most noteworthy osteological and external morphological characteristics of *P. dorsalis*, which are autapomorphies in the Sisoroidea or key features distinguishing it from known amblycipitids. The evolutionary significance of these features as apomorphies, plesiomorphies or homoplasies are assessed in the Sisoroidea in reference to Big Asia clade.

Anterior truncation of infraorbital canal and infraorbital bones (Figs. 4a, 11a, 11b). In siluriforms, the infraorbital bones comprise several tubular ossicles surrounding the eye plus lacrimal (the first infraorbital). The infraorbital canal runs through these bones which are referred to as infraorbital (circumorbital) series. The infraorbital series is plesiomorphically complete in most catfishes. Even catfish that have completely lost their eye, such as the ictalurids (Lundberg, 1982; Lundberg et al., 2017) and the heptapterids (Bockmann and Castro, 2010) possess a complete infraorbital series surrounding the orbit region. On other hand, the absence or truncation of the infraorbital series is observed in a few eyed catfishes. For example, the infraorbital series is absent in the eyed kryptoglanids (Britz et al., 2014; Lundberg et al., 2014) and the infraorbital bones are reduced to the posteriormost element but with lacrimal in South American trichomycterids (Arratia and Huaquin, 1995; Rizzato and Bichuette, 2017). Thus, the anterior truncation or complete loss of infraorbital bones (and infraorbital

canal) is a character with phylogenetic significance rather than a regressive trait related to subterranean life.

The infraorbital series is complete in all catfishes of the Big Asia clade except for *Proliobagrus*. In *P. dorsalis*, the infraorbital series is reduced to the lacrimal and the posteriormost infraorbital bone (Fig. 4a). The infraorbital canal is anteriorly truncated, leading to a segment passing through the posteriormost tubular infraorbital, then transforming to a short cartilaginous canal terminating at a pore (Figs. 11a, 11b). The anterior truncation of infraorbital canal in *P. dorsalis* is an autapomorphy distinguishing it from all other sisoroid genera.

First dorsal-fin pterygiophore compressed with lack of canal, anteriorly fused with a forward process (Figs. 2, 9). In most siluriforms, the first dorsal-fin pterygiophore (proximal radial) is a laminar ossicle with transverse lamina at the dorsal end which forms the middle nuchal plate (Mo, 1991). The transverse lamina can possess a pair of posteriorly extending wing that forms a semicircular structure for transmitting the tendons of the erector muscles of the short spine (Lundberg, 1970). In some catfish, a pair of bony canals (Fig. 14d) develops at the dorsal part of the first pterygiophore through which run the erector muscles (termed as “muscle canal” in Chen, 1994), thus first dorsal-fin pterygiophore is a three-dimensionally complex ossicle. The paired bony canals (Figs. 14d, 15b) develop in the Amblycipitidae (Chen, 1994. Figs. 22, 24), Akysidae (Chen, 1994. Fig. 23), and some sisorid species (Zhou W. and Zhou Y., 2005. Fig. 7). Furthermore, the anterior end of the first dorsal-fin pterygiophore is modified as an expanded depression in the Amblycipitidae (Fig. 14d) (Chen, 1994. Figs. 22, 24). This anterior expanded depression is observed in *Akysis vespa* but not in *Breitensteinia insignis* (Chen, 1994. Fig. 23), and it was not examined or reported in other species of the Akysidae. In the Sisoridae, the first dorsal-fin pterygiophore is three-dimensionally with paired bony canal in most genera but the bony canals absent in some glyptosternines (He, 1996. Fig. 22). However, the anterior depression is weakly developed in some glyptosternines such as that in *Oreoglanis delacouri* (Fig. 16d).

Within the Big Asia clade, the first dorsal-fin pterygiophore is a laminar ossicle lacking an anterior depression (but with a semiring for transmitting the erector muscle of spinelet) in bagrid genera (Mo, 1991), and also in the Diplomystidae which is the most basal lineage in siluroidei, we therefore interpret that a compressed laminar-like first dorsal pterygiophore is plesiomorphic whereas the presence of an anterior depression is considered apomorphic for the Sisoroidea. In *P. dorsalis*, the first dorsal-fin pterygiophore is a compressed laminar ossicle with neither paired bony canals nor a semiring for the erector muscles. It additionally has a prominent anterior process (Figs. 9a, 9c) which we suspect as a consequence of anteriorly fusing with a reduced supraneural. Thus, the first dor-

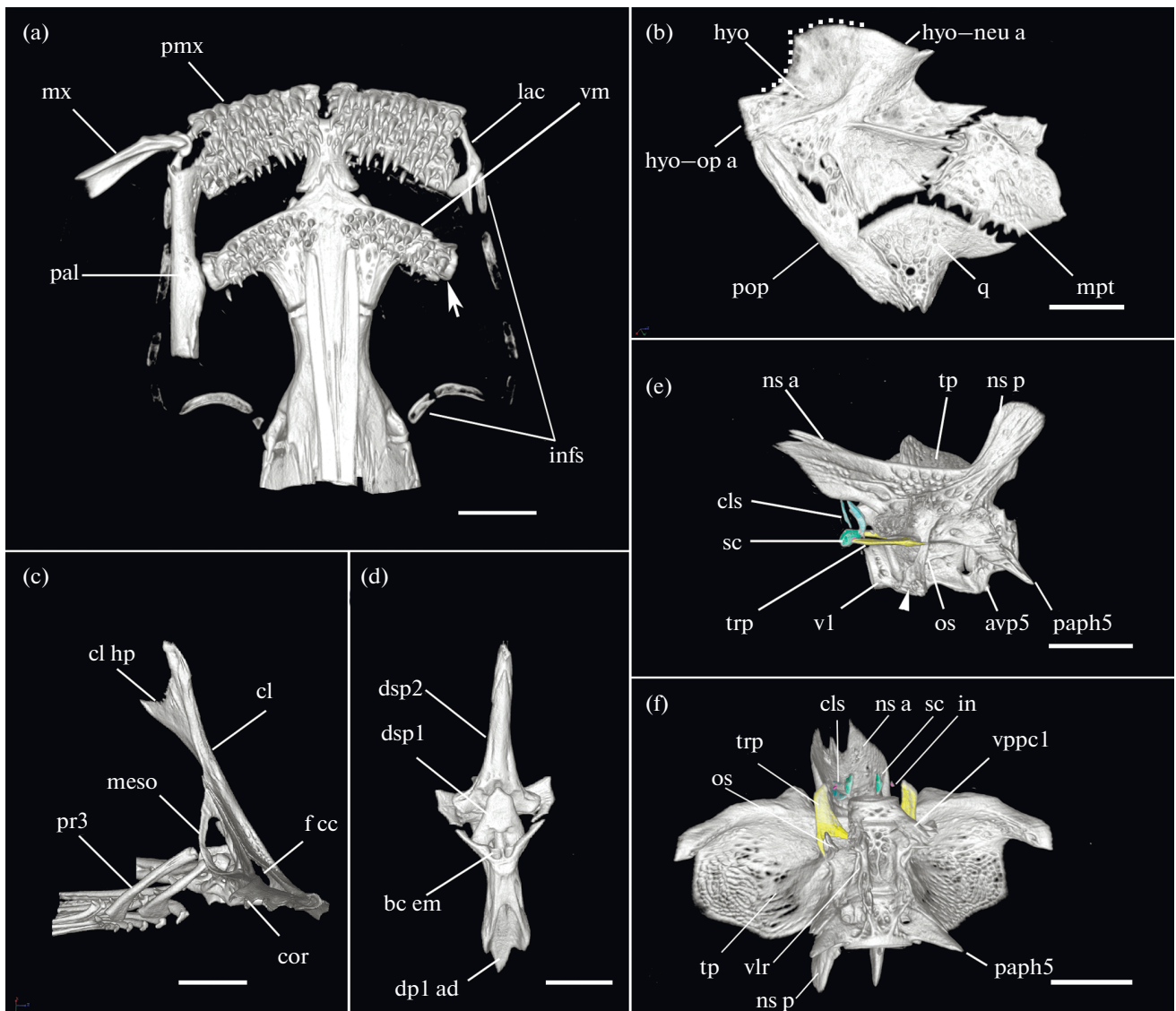


Fig. 14. Comparative materials from *Xiurenbagrus gigas* LJH 02040108: (a) snout in ventral view with left autopalatine and maxilla removed, (↔) vomer approaching to lateral margin of the lateral ethmoid; (b) right suspensorium in lateral view, (···) the margin of posterodorsal expansion of the hyomandibula; (c) left pectoral girdle in medial-oblique view, (d) first dorsal-fin pterygiophore and dorsal spine in anterior view, (e) Weberian apparatus in lateral view (rostral end to left) with left transverse lamina removed, (◄) the joint among posteroventral process of vertebra 1, ventrolateral process of compound Weberian centrum, and ventral end of ossified suspensorium; (f) Weberian apparatus in ventral-oblique views (rostral end to up) with right ventroposterior process of centrum 1 and associated anterior ventrolateral ridge of compound Weberian centrum removed.

avp5, anteroventral process of vertebra 5; bc em, bony canal for erector muscles; dp1 ad, anterior depression of first dorsal-fin pterygiophore; dsp 1, 2, first, second dorsal spine; cl, cleithrum; cl hp, humeral process of cleithrum; cls, claustrum; cor, coracoid; f cc, foramen between cleithrum and coracoid; hyo, hyomandibula; hyo-neu a, articular facet of hyomandibula for neurocranium; hyo-op a, articular facet of hyomandibula for opercle; in, intercalarium; infi, infraorbitals; lac, lacrimal; meso, mesocoracoid; mpt, metapterygoid; mx, maxilla; ns a, anterior neural spine of the compound Weberian centrum; ns p, posterior neural spine of the compound Weberian centrum; os, ossified suspensorium; pal, autopalatine; paph5, paraphysis 5; pmx, premaxilla; pop, preopercle; pr 3, pectoral proximal radial 3; q, quadrate; sc, scaphium; trp, tripus; tp, transverse process of the compound Weberian centrum; v1, vertebra 1; vlr, ventrolateral ridge of the compound Weberian centrum; vm, vomer; vppc1, ventroposterior process of centrum 1. Scale: 2 mm.

sal-fin pterygiophore of *P. dorsalis* is derived from a plesiomorphic state with a unique anteriorly directed process. Such a feature is an autapomorphy in the Sisoroidea.

Moreover, there is no fin spine supported by the first pterygiophore, thus “the first dorsal-fin spine (spinelet)” is absent in *P. dorsalis*, and the middle radial of first dorsal-fin pterygiophore extends into the

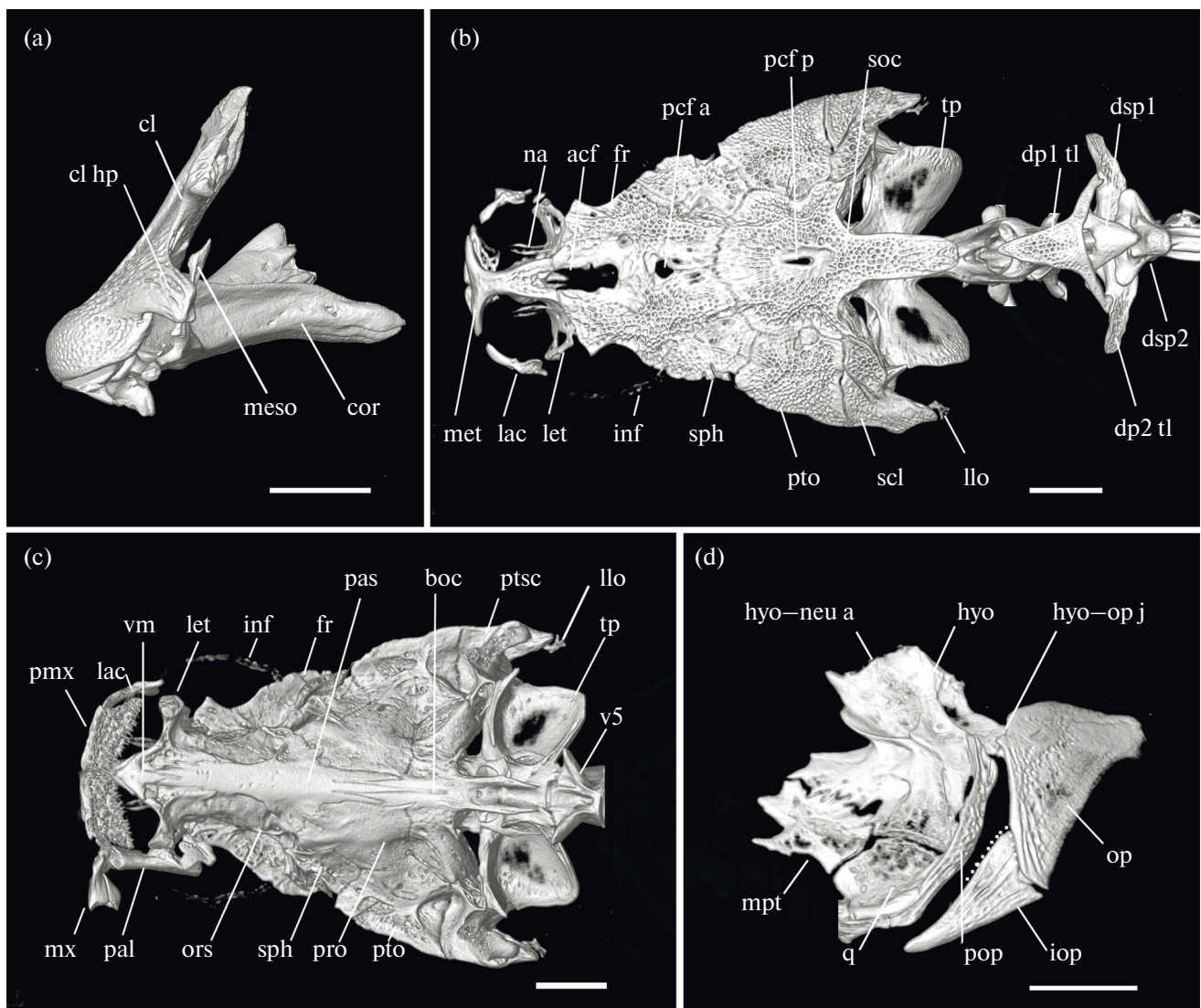


Fig. 15. Comparative materials from *Akysis vespa* KIZ 3473: (a) left pectoral girdle in posterior view, (b) skull roof with associated anterior vertebrae in dorsal view, (c) neurocranium plus the right autopatine and maxilla and the Weberian apparatus in ventral view, (d) left suspensorium and operculum in lateral view; (···) the margin of posterodorsal intension of interopercle in (d). boc, basioccipital; cl, cleithrum; cl hp, humeral process of cleithrum; cor, coracoid; dp1 tl, transverse lamina of first dorsal-fin pterygiophore; dp2 tl, transverse lamina of second dorsal-fin pterygiophore; dsp 1, 2, first, second dorsal spine; fr, frontal; hyo, hyomandibula; hyo-neu a, articular facet of hyomandibula for neurocranium; hyo-op j, hyomandibula-opercle joint; inf, infraorbital; iop, interopercle; lac, lacrimal; let, lateral ethmoid; llo, lateral line ossicle; met, mesethmoid; meso, mesocoracoid; mpt, metapterygoid; mx, maxilla; op, opercle; na, nasal; ors, orbitosphenoid; pal, autopatine; pas, parasphenoid; pcf a, anterior subdivision of posterior cranial fontanelle; pcf p, posterior subdivision of posterior fontanelle; pmx, premaxilla; pop, preopercle; pro, prootic; pto, pterotic; scl, supracleithrum; q, quadrate; sph, sphenotic; soc, supraoccipital; tp, transverse process of the compound Weberian centrum; vm, vomer; v5, vertebra 5. Scale: 2 mm.

articular foramen of the second dorsal spine to form a bony bridge (Fig. 9c) by fusing with the distal end of second dorsal-fin pterygiophore. Within the Sisoroidea, this condition is also present in some glyptosternines (He, 1996; Fig. 22; *Pareuchiloglanis* species we examined). We consider this similarity to be due to a convergence.

Dorsal fin posteriorly displaced and first dorsal-fin pterygiophore situated apart from the compound vertebra (Fig. 2). In most catfishes, the dorsal fin is subse-

quent to the skull roof and the first dorsal-fin pterygiophore usually attaches to the fourth to sixth neural spine (Mo, 1991). In the Diplomystidae and some bagrid genera, the first dorsal-fin pterygiophore inserts a position between fifth and sixth neural spines and does not contact with the fourth neural spine (the posterior neural spine of the compound Weberian vertebra), but inserts into bifid fourth neural spine in *Horabagrus*, *Rite rita* and some bagrid genera. In the Amblycipitidae and the examined species of Akysidae,

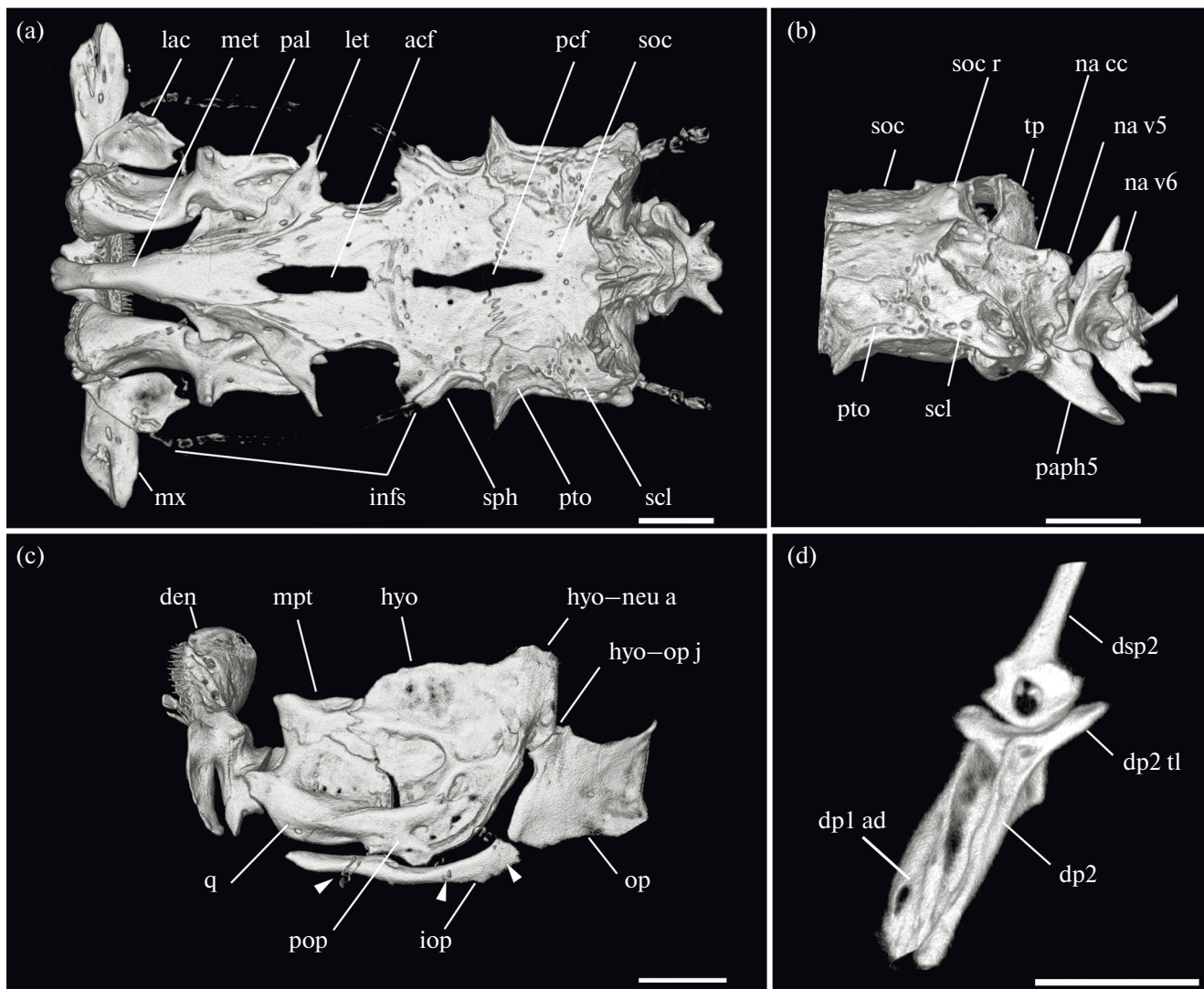


Fig. 16. Comparative materials from *Oreoglanis delacouri* YU 20100514024: (a) skull roof plus upper jaw and autopalatine in dorsal view, (b) posterior skull plus anterior vertebrae in lateral view the superapreopercle canal removed, (c) left suspensorium and operculum plus low jaw in lateral view (superapreopercle canal removed), (d) first and second dorsal-fin pterygiophores and associated elements in oblique view.

acf, anterior cranial fontanel; na cc, neural arch of the compound Weberian centrum; den, dentary; dp1 ad, anterior depression of first dorsal-fin pterygiophore; dp2, second dorsal-fin pterygiophore; dp2 tl, transverse lamina of second dorsal-fin pterygiophore; dsp 2, second dorsal spine; hyo, hyomandibula; hyo-neu a, articular facet of hyomandibula for neurocranium; hyo-op j, hyomandibula-opercle joint; infs, infraorbitalis; iop, interopercle; lac, lacrimal; let, lateral ethmoid; met, mesethmoid; mpt, metapterygoid; mx, maxilla; pto, pterotic; scl, supracleithrum; q, quadrate; soc, supraoccipital; soc r, supraoccipital crest; sph, sphenotic; na v5, neural arch of vertebra 5; na v6, neural arch of vertebra 6; (◀) the branches of sensory canal in preopercle in (c). Scale: 2 mm.

first dorsal-fin pterygiophore directly attaches to the fourth neural spine, whereas the insertion place varies in the Sisoridae, ranging from a position between the fourth and fifth, or the fifth and sixth neural spine, to that posterior to the six neurals. In *P. dorsalis*, dorsal fin is posteriorly placed and first dorsal-fin pterygiophore inserting into the bifid neural spine of vertebra 10 and apart from the compound vertebra (the Webe-

rian complex), which distinguishes this fish from all known amblycipitid genera.

Compound vertebra of Weberian apparatus (Fig. 7). In siluriforms, the Weberian apparatus is comprised of Weberian complex (pars sustentaculum) including vertebrae 1–4 (with vertebra 5 more or less incorporated in some catfishes) and Weberian ossicles (pars auditum). We first discuss four characters of Weberian

complex of *P. dorsalis* in this section: (1) first vertebra; (2) ventral median ridge of compound vertebra; (3) auxillary parapophysis of fourth vertebra; (4) fourth neural spine dorsoventrally bifurcated; before discussing the Weberian ossicles in next section.

(1) In catfish, first vertebra is autogenous or fused with the Weberian compound vertebra. In the Diplostomidae, first vertebra is a thin disc centrum without any processes. In the bagrid genera examined, there is a pair of ventroposterior process on the first vertebra, which articulate with the anterior end of paired ventrolateral flanges of the compound vertebra. In the three examined species of the Akysidae, the first vertebra is not visible which seems to fuse with the compound vertebra. In the all examined genera of the Sisoridae, the first vertebra is thin disc without any process except *Bagarius yarrelli* in which first vertebrae fuses with the compound Weberian centrum. In the Amblycipitidae, there is variance on the ventroposterior process of first vertebra. In genera *Liobagrus*, *Xiurenbagrus*, first vertebra has paired ventroposterior processes articulating with the the anterior end of paired ventrolateral flanges of compound vertebra. In genus *Amblyceps*, the process is absent at least in *Amblyceps mangensis* (Tilak, 1967. Fig. 2). In *P. dorsalis*, first vertebra is a thin disc-like centrum without any process, which is similar to that in the Sisoridae and *Amblyceps mangensis*.

(2) In the Amblycipitidae, the second to fourth vertebrae are fused to form the Weberian compound vertebra. A pair of ventrolateral ridges flanks the aortic groove (Fig. 14f) (Chen, 1994), which joins anteriorly with the ventroposterior process of first vertebra (if present) and posteriorly with the anteroventral process of fifth vertebra (Fig 14f; Chen, 1994. Fig. 62). In *Xiurenbagrus* (Fig. 14) and *Liobagrus* species we examined, the os suspensorium extends ventrally and reaches the joint between posteroventral process of first vertebra and the ventrolateral ridge of the compound vertebra. The presence of the paired ventrolateral ridges awaits a thorough investigation in the Akysidae and Sisoridae, although it has been reported in some species, such as the akysids *A. vespa* (Fig. 15c), and the sisorids *Pseudechis sulcatus* (Gauba, 1968. Fig. 2), *Glyptosternum maculatum* (He, 1996. Fig. 2). However, it is absent in *Glyptothorax cavia* (Gauba, 1966. Fig. 2) and *Pareuchiloglanis* (He, 1996. Fig. 15). In the context of the Big Asia clade, the paired ventrolateral ridges flanking aortic groove is present in bagrid genera (Mo, 1991; Tilak, 1965; Zhang and Wang, 1995) and the Diplomystidae (Arratia, 1987), and we therefore interpret the presence of paired ventrolateral ridges flanking the aortic groove as plesiomorphic in the Sisoroidea. In *P. dorsalis*, an evident ventral median ridge (Fig. 7a) rather than paired ventrolateral ridges is present and the aortic is located to the left of it; the os suspensorium extends antero-obliquely (Fig. 7b); the fifth vertebra lacks an anteroventral process. The

presence of a ventral median ridge instead of paired ventrolateral ridges distinguishes *P. dorsalis* from all known amblycipitid genera and many other sisoroid genera.

(3) In the Akysidae, Amblycipitidae, and Sisoridae, the compound vertebra has a pair of sheet-like transverse processes extending from the compound Weberian centrum (modified into a bony capsule in some sisorid species), as in most catfishes. They are putatively parapophyses of the fourth vertebra. In *P. dorsalis*, a small separate process posterolaterally extends from the compound vertebra following the transverse process (Figs. 7b, 7e). We interpret it as an auxillary parapophysis from the fourth vertebra, and consider it as an autapomorphy in the Sisoroidea.

(4) In the Akysidae, Amblycipitidae, and Sisoridae except glyptosternine (Fig. 16b), there is a pair of posterior neural spines on the compound vertebra, the fourth neural spine (Chen, 1994; de Pinna, 1996; Ng, 2010, 2015). In *P. dorsalis*, the fourth neural spine is significantly modified. Each half of fourth neural spine is bifurcated dorsoventrally (Fig. 7e), and a heavy strut-like process extends ventrally off the base of each half of the fourth neural spine. It is considered an autapomorphy in the Sisoroidea.

Weberian ossicles: absence of claustrum, scaphium lack of ascending process, and outward extended transformator process of tripus (Fig. 7). In siluriforms, there are either three or four pairs of Weberian ossicles: claustrum, scaphium, interclarium, and tripus (Chardon et al., 2003). The presence of claustrum is considered plesiomorphic in siluriforms (Chardon et al., 2003). The claustrum is reported to be present in the Amblycipitidae (Tilak, 1967. Fig. 5; Mo, 1991), but absent in the Akysidae and Sisoridae (Tilak, 1963; Mo, 1991). Our investigation confirmed the absence of claustrum in species of the Akysidae and Sisoridae, and the presence of claustrum in *X. gigas* (Fig. 14e). The claustrum is a vertical, elongate bone, thinner than ascending process of the scaphium if it present. We were unable to find the claustrum in the microCT data of *Labeo anguillicauda* specimens, which might be due to unossification of the bone or much thinner than the spatial resolution imaging data. As the claustrum is present in the Diplostomidae and bagrid genera (Tilak, 1965; Zhang and Wang, 1995), the absence of the claustrum is interpreted as apomorphic in the Sisoroidea. In *P. dorsalis*, the claustrum is absent which distinguishes this species from amblycipitid genera but not from akysids and sisorids.

The scaphium may possess an ascending process in catfish. Chardon et al. (2003) reported the presence of an ascending process in the Amblycipitidae (Tilak, 1967), but the absence of an ascending process of scaphium in the Akysidae and Sisoridae (illustrated in *Gagata*, *Glyptothorax lonah*, *Nangra* by Tilak, 1963. Figs. 49, 52, 59). It is noteworthy that a scaphium with an ascending process has been illustrated in *Glyptosternon*

nium reticulatum (Tilak, 1963. Fig. 75). Our investigation confirmed the presence of an ascending process on the scaphium in *X. gigas* (Fig. 14e), *Amblyceps yunnanis* and *Liobagrus* species, but absence in the examined sisorid species except *Glyptosternum reticulatum*. Within the Big Asia clade, the scaphium possesses an ascending process in bagrid genera (Tilak, 1965. Figs. 27, 28, 34, 40, 43, 47; Zhang and Wang, 1995. Fig. 1). Thus, the absence of ascending process of scaphium is interpreted as apomorphic in the Sisoroidea. In *P. dorsalis*, the scaphium lacks an ascending process (Fig. 7b) which again distinguishes this species distinguished from other amblycipitid genera.

The tripus is the largest of the Weberian ossicles. It is roughly crescent-shaped in many catfishes (Tilak, 1965. Figs. 29, 30, 35, 41, 42, 48; Zhang and Wang, 1995. Fig. 1) with a convex or straight lateral margin, and a medially curved transformator process. Such tripus has reported in amblycipitid species *A. mangois* (Tilak, 1967. Fig. 5), *X. gigas* (Fig. 14f), *Liobagrus* species we examined, and *Akysis vespa* (Fig. 15c). Mo (1991) reported the transformator process of the tripus to curve laterally in the Sisoridae. It was illustrated in *Sisor rhabdophorus* (Mahajan, 1967. Figs. 1, 5), *Glyptothorax lonah* (Tilak, 1963. Fig. 60) which displays a front-to-rear flipped version of that in *P. dorsalis* (Fig. 7a), however the tripus has a gently straight or convex lateral margin in *Bagarius bagarius* (Tilak, 1963. Fig. 68), *Eretistes pusillus* (Gauba, 1967. Fig. 3), and *Gagata gagata* (Tilak, 1963. Fig. 64). Our investigation also suggested there is a variation on the configuration of the transformator process of the tripus in the Sisoridae. Here, we consider an outwardly extended transformator of the tripus is apomorphic in the Sisoroidea. It is noteworthy that the transformator processor of tripus in *Amblyceps yunnanensis* extends outward in our examined specimens. In *P. dorsalis*, the tripus has a strongly concave lateral margin, and is significantly modified with a predominantly outwardly extended transformator process (Fig. 7a). Given the morphology, the Weberian ossicles of *P. dorsalis* distinguish it from all known amblycipitid genera.

Incomplete mesocoracoid arch (Figs. 10d, 10e). In many catfishes, the dorsal and ventral ends of the mesocoracoid are fuses with the posterodorsolateral and posteroventrolateral surfaces of the coracoid respectively, thus forming a “mesocoracoid arch” (Diogo et al., 2001). It has been reported that the mesocoracoid arch is well developed in the Amblycipitidae and Sisoridae (Chen, 1994; Diogo et al., 2003; Ng, 2015), but it is incomplete as the dorsal end of the mesocoracoid is separate from the coracoid in the Akysidae, which were recorded in *Acrochordonichthys*, *Breitensteinia*, *Parakysis* (Mo, 1991) and other *Akysis* species (Friel, 1994). Our investigation confirmed that the mesocoracoid arch is complete in the Amblycipitidae and Sisoridae, but is incomplete in *Akysis vespa* (Fig. 15a) in which the mesocoracoid is an ascending process dorsally separated from the cora-

coid. In one *Akysis vespa* specimen and *Pseudobagrus hardmani*, the dorsal part of the mesocoracoid bears a short, mesidally directed process which is attached to the medial side of the coracoid. This is contrary to “a complete mesocoracoid arch” in the Amblycipitidae, as the dorsal end is fused with the coracoid in *X. gigas* (Fig. 14c) but it is free in *Akysis* and *Pseudobagrus*. In the Diploymitidae and other members of the Big Asia clade, the mesocoracoid arch is complete except in *Rita* and *Nanobagrus* (Mo, 1991), thus we interpret an incomplete mesocoracoid arch as a derived condition in the Sisoroidea. In *P. dorsalis*, the mesocoracoid arch is incomplete as the mesocoracoid is a well-developed ascending process with a bifid dorsal tip separating from the the coracoid (Figs. 10d, 10e). It is apomorphic in the Sisoroidea. This trait distinguishes *P. dorsalis* from all known amblycipitid genera, and may suggest a close relationship between *P. dorsalis* and the Akysidae.

Anterior fontanelle closed and posterior fontanelle subdivided into two (Fig. 3a). Catfishes begin cranial development with just two fontanelles (anterior and posterior) along the midline of skull roof that are separated by the epiphyseal bar. The longitudinal subdivisions of posterior fontanelle can result from development on new midline joints. In the Amblycipitidae, anterior and posterior fontanelles are narrow longitudinal open, and the paired frontals flank both fontanelles and have no contact with each other except at the epiphyseal bar (Chen and Lundberg, 1995. Fig. 4; Sun, 2011. Fig. 4-1). The anterior fontanelle reaches or extends anteriorly to the mesethmoid, whereas the posterior fontanelle extends posteriorly to supraoccipital (giving it a deep median notch). Given this configuration is present in the Diplomystidae and widespread in majority of bagrids (Mo, 1991. Fig. 6; Zhang et al., 1995. Figs. 1, 2), we interpret it as plesiomorphic within the Big Asia clade. In the Akysidae and Sisoridae, anterior fontanelle is the same as that in amblycipitids, but a longitudinal subdivision of posterior fontanelle frequently develops. In *Akysis verspa* (Fig. 15b), the paired frontals join again medially and subdivides the posterior fontanelle into a foramen-like anterior portion posterior to the epiphyseal bar and a posterior portion wholly enclosed in the supraoccipital, and this condition was also illustrated for *Breitensterinia insignis* (de Pinna, 1996. Fig. 10). In the Sisoridae, the subdivision of the posterior fontanelle is frequently occurred. The posterior portion of the posterior fontanelle is wholly enclosed in the supraoccipital in *Bagarius sp.* (Chen, 1994. Fig. 6; He, 1996. Fig. 14; Zhou W. and Zhou Y., 2010. Fig. 6a), *Glyptothorax sp.* (He, 1996. Fig. 14; Vishwanath et al., 2010. Fig. 5; Zhou W. and Zhou Y., 2010. Fig. 6b), and *Eretistes pusillus* (Chen, 1994. Fig. 7), whereas it is framed by the paired frontals and the supraoccipital in glyptosternoid *Glaridoglanis*, *Exostoma*, and some *Pareuchiloglanis* species (He, 1996. Fig. 14).

In *P. dorsalis* (Fig. 3a), the anterior fontanelle is completely closed as paired frontals meeting each other anterior to the epiphyseal bar, and the posterior fontanelle is subdivided into an aperture-like anterior opening subsequent to the epiphyseal bar and a wide posterior opening mainly located at the supraoccipital and anteriorly flanked by the posterior margin of the frontal. The complete closure of anterior fontanelle is an autapomorphy among the Sisoroidea. The subdivision of posterior fontanelle distinguishes this species from all known amblycipitid genera.

First proximal pectoral radial cartilage roughly round (Fig. 12c). In members of the Big Asia clade including sisoroids (Mo, 1991; de Pinna, 1996), the first proximal pectoral radial is plesiomorphically an approximately round-shaped cartilaginous structure that is modified into an elongated form in the Amblycipitidae and akysid genus *Parakysis* (de Pinna, 1996. Fig. 31). In *P. dorsalis* (Fig. 12c), the first proximal pectoral radial is approximately round-shaped which distinguishes it from the condition in amblycipitids.

Fewer procurent caudal-fin rays (Fig. 9f). In most catfishes, the procurent caudal-fin rays remain unchanged from juvenile to adult stages (Arratia, 2003a). Chen (1994) examined the procurent caudal-fin rays of the Amblycipitidae. The mean count of ventral (lower) procurent rays ranges from 12.7 to 19.0 (Chen, 1994) and the anteriormost ray reaches the tip of haemal spine of the preural centrum 8, whereas the mean count of dorsal (upper) procurent rays is 14.0–22.7 (Chen, 1994) with the anteriormost ray reaching the tip of neural spine of preural centrum 8. In *P. dorsalis* (Fig. 9f), there are eight ventral procurent caudal-fin rays with the anteriormost two anterior to the tip of haemal spine of preural centrum 5, and eight dorsal procurent rays with the anteriormost two anterior to the tip of neural spine of preural centrum 4. Although the distribution of counts of procurent caudal-fin rays has not been thoroughly investigated among the Sisoroidea in a phylogenetic context, the fewer ventral and dorsal procurent rays distinguish *P. dorsalis* from the all known amblycipitid genera.

Foramen closed framed by orbitosphenoid and pterosphenoid (Fig. 3c). In catfish, exit foramen or foramina for the optic, trigeminal and facial nerves sit on the orbit wall of neurocranium (Arratia, 2003b). In the Diplomystidae, there is only one foramen for these three group nerves framed by the orbitosphenoid anteriorly, pterosphenoid dorsally, prootic posteriorly, and the parasphenoid ventrally, and the pterosphenoid doesn't contact with the parasphenoid. In the Bagridae, a process extends ventrally from the pterosphenoid and reaches the parasphenoid to form a bony septum, thus two foramina are formed: anterior one is supposed to be exit for optic nerve and the posterior one for trigeminal and facial nerves. In the superfamily Sisoroidea, there are usually three exit foramina because an independent foramen for facial nerve is

formed due to a second process being extended ventrally from the pterosphenoid, or a ventral process extending from the anterior part of the sphenoid. In most bagrids and sisoroids, the exit foramen for optic nerve is framed by orbitosphenoid anteriorly and pterosphenoid posteriorly, with involvement of the parasphenoid ventrally in some cases, as illustrated in *Glyptosternum maculatum* (He, 1996. Fig. 3), *Glyptosternum reticulatum* (Tilak, 1963. Fig. 42), *Sisor rhabdophorus* (Mahajan, 1966. Fig. 3), *Gagata sexualis* (Ng, 2015. Fig. 1), *Glyptothonax lonah* (Tilak, 1963. Fig. 19), *Pseudecheneis sulcatus* (Gauba, 1968. Fig. 2), and akysid species *Akysis vespa* (our observation). However, in *P. dorsalis* (Fig. 3c), the foramen framed by the orbitosphenoid and pterosphenoid is closed to a rudimentary aperture. Such closed optic foramen is also observed in *Bagarius yarrelli* and *Acrochordonichthys rugosus*, and this optic foramen is significantly reduced in *Akysis vespa*. On other hand, the optic foramen is present in blind ictalurid cave catfishes (Lundberg, 1982. Fig. 7; Lundberg et al., 2017. Fig. 4). Thus, this aperture remnant seems not to be related to subterranean life in *P. dorsalis* but to independently evolve in the superfamily Sisoroidea.

External Morphology

Xiu et al. (2014) have described some external morphological characters to distinguish *Proliobagrus* from all other amblycipitid genera. We describe two additional onesunreported in the previous study.

Base of nasal barbel on the anterior margin of posterior nostril (Fig. 13a). In the Amblycipitidae, the anterior nostril is located at the end of a short tube or valve, whereas a flap is present on the posterior nostril and is confluent with the base of the nasal barbel (Chen, 1994. Fig. 76), making the opening of posterior nostril a narrow longitudinal slit (Figs. 13b–13d). In the Akysidae, the two nostrils are separated, with the anterior nostril at the end of a short tube (except in *Pseudobagarius*) and the base of nasal barbel is immediately adjacent to the anterior margin of the posterior nostril (Ng and Kottelat, 1998b. Fig. 4; 2003. Fig. 2; Ng H. and Ng P., 2001. Fig. 1). In *P. dorsalis* (Fig. 13a), both anterior and posterior nostrils lack a flap, and the base of the nasal barbel is immediately adjacent to the anterior margin of posterior nostril. Although the phylogenetic significance of this character is unclear, it distinguishes *P. dorsalis* from the other amblycipitid genera.

Presence of widely exposed pseudotympanum (Figs. 1a, 2a). The pseudotympanum is an externally visible anterior portion of the swim bladder in the body wall created by reduction of the hypaxialis muscle (Birindelli and Shibatta, 2011; Dutra et al., 2015). Plesiomorphically, it is absent in members of the Big Asia clade including the Sisoroidea (except *Ayarnangra estuaricus* — Roberts, 2001). On other hand, a widely exposed pseudotympanum has been reported in some

troglobitic catfishes, such as *Rhamdiopsis krugi* (Bockmann et al., 2010. Fig. 13), *Phreatobius* spp. (Shibatta et al., 2007; Muriel-Cunha, 2008; Ohara et al., 2016), and *Horaglanis* spp. (Babu, 2012; Vincent, 2012). Given that the swimbladder is expanded and touches the body wall can enhance sensation of sound vibration in lentic environments (Kratochvil and Ladich, 2000), we consider the pseudotympanum in blind cavefishes as a troglomorphic (adaptive to subterranean life) trait compensating for visual loss. In *P. dorsalis*, the transverse bilobed swimbladder is large, each sac of which reaches body wall and is visible externally; this trait is a potential constructive troglomorphic character.

Review of Synapomorphies of the Amblycipitidae

Chen (1994) performed a comprehensive morphological analysis of the Amblycipitidae, which has hitherto been “the latest” comprehensive osteological investigation, and proposed three “unique” (the first three characters in the following account) and three “non-unique but unambiguous” synapomorphies for the Amblycipitidae (see also Chen and Lundberg, 1995). Sullivan et al. (2008) performed most recent molecular phylogenetic study of the Amblycipitidae, and generated a diphyletic tree in which *Amblyceps* is sister to the Sisoridae and the other clade is comprised of (*Liobagrus* + *Xiurenbagrus*) and the Akysidae. They reviewed the systematic studies of the Amblycipitidae, and thought “both data sources ... offer robust evidence” (Sullivan et al., 2008. P. 98). Here, we re-examined those features, and suggested not only that the previously proposed “synapomorphies” was occur in other sisoroids but that evident disparities of several characters are present in three genera of the Amblycipitidae.

(1) An enlarged posterodorsal portion of hyomandibula (Chen, 1994. Figs. 16b, 43–47; Chen and Lundberg, 1995. Fig. 2). Chen (1994) reported that the posterodorsal portion of the hyomandibula (posterior to a vertical ridge extending ventrally from the hyomandibula-neurocranium joint to the bone’s center and dorsal to the horizontal ridge extending to the hyomandibula-opercular joint) was well developed in the Amblycipitidae (Chen, 1994. Figs. 43–47), and a smaller posterodorsal portion was present in akysids *Akysis leucorhynchus*, *Acrochordonichthys melanogaster* (Chen, 1994. Fig. 16A) and sisorids species *Euchiloglanis kodgarti* (Chen, 1994). We agree that an expanded posterodorsal portion of hyomandibula is derived as it is absent in the Diplomystidae and Bagridae. However, this posterodorsal expansion was reported in some glyptosternines such as *Pareuchiloglanis sinensis*, *Pseudexostoma* sp. (He 1996. Fig. 18), and our survey indicated that evident posterodorsal expansion is present in some sisorids such as *Bagarius yarrelli*, *Nangra nangra*, although it is absent in other sisorids (Mahajan, 1966. Fig. 2; He, 1996. Fig. 18;

Guba, 1966. Figs 1, 4; 1967, Fig. 1; 1968. Figs. 1, 4). Chen (1994. P. 39) combined two states, “presence of posterodorsal portion but small” and “absence of posterodorsal portion”, into his state 0 “laterodorsal portion of hyomandibula very small with irregular shape”, treating the development of posterodorsal portion as unique for the Amblycipitidae. Furthermore, the morphology of the free margin of this posterodorsal portion varies within genera of the Amblycipitidae. It is gently convex in *Amblyceps* (Tilak, 1966. Figs. 1, 2; Chen, 1994. Figs 16B, 43, 45, 46) but bears a deeply concave notch in *Liobagrus* and *Xiurenbagrus* (Fig. 14b) (Chen, 1994. Fig. 47; Chen and Lundberg, 1995. Fig. 2C). A convex posterodorsal margin is present in sisoroid species such as *Bagarius yarrelli*, *Pareuchiloglanis sinensis*, while a deeply notched posterodorsal margin is illustrated in akysid species *Akysis vespa* (Fig. 15d) and *Acrochordonichthys melanogaster* (Chen, 1994. Fig. 16A). Therefore, the phylogenetic significance of this character is limited. *Proliobagrus dorsalis* has a prominent posterodorsal expansion of hyomandibula with a gently convex free margin (Figs. 5b, 5c), a condition similar to that in *Amblyceps* but different from that in *Liobagrus* and *Xiurenbagrus* (Fig. 14b).

(2) Narrow posterodorsal extension of the interopercle (Chen, 1994. Figs. 17, 48), with its posterior margin matching the convex anteroventral margin of the opercle. The interopercle is roughly triangular and posteriorly deeper with a truncate or convex posterior margin in catfishes. In the Amblycipitidae, the posterior margin of the interopercle is concave and closely matches the anteroventral margin of the opercle, bearing a posterodorsal extension (Chen, 1994. Figs. 17, 48). Our survey suggested that the posterior margin of the interopercle is either truncate (Guba, 1966. Fig. 13) or roughly convex (Fig. 16c) (He, 1996. Fig. 18), and does not match the anteroventral margin of the opercle in the Sisoridae, and it is roughly convex in akysid species *Pseudobagarius hardmani* and *Acrochordonichthys rugosus* but a short posterodorsal extension of the interopercle is present in *Akysis vespa* (Fig. 15d). In the Big Asia clade, a posterodorsal extension of interopercle matching the convex anteroventral margin of the opercle is also present in the bagrids *Bagrus bayad*, *Bagrus docmak*, *Hemibagrus macropterus*, *Hemibagrus nemurus*, *Laide hexanema*, and *Mystus gulio* (Mo, 1991. Figs. 14, 46, 52). Thus, phylogenetic significance of the posterodorsal extension of interopercle is limited. *Proliobagrus dorsalis* has an interopercle with concave posterior margin matching the anteroventral margin of the opercle, bearing a short posterodorsal extension (Fig. 5e).

(3) Oblique orientation and deep subcutaneous position of the middle nuchal plate (Chen, 1994. Figs. 22a, 22c, 24; Sun, 2011). In the Amblycipitidae, the first dorsal pterygiophore contacts the fourth neural spine (posterior neural spine of the compound Weberian centrum), with the middle nuchal plate

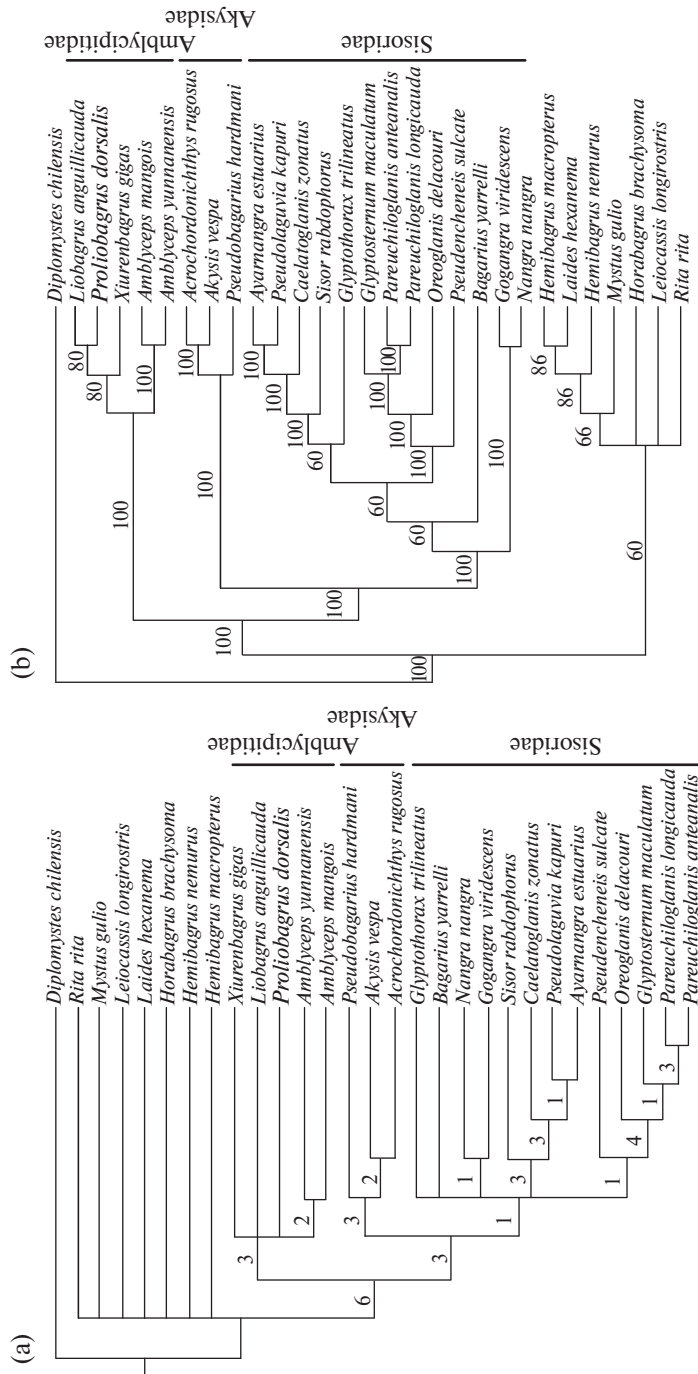


Fig. 17. Strict consensus and majority rule trees for 15 most parsimonious trees produced by the analysis of the matrix of 29 taxa coded for 68 morphological characters. Numbers above and below the branches correspond to Bremer support and Bootstrap values.

(transverse lamina of the first pterygiophore) deeply embedded in the body. We were unable to ascertain the corresponding character state in *P. dorsalis*, as the dorsal fin is posteriorly placed and locates far from the Weberian complex (Figs. 1, 2, 9a–9d), even though the transverse lamina of first pterygiophore is embedded in the body.

(4) Fusion of the basal elastic cartilages of the inner and outer mental barbels in a “head-to-tail” connection pattern (Chen, 1994. Fig. 30; Chen and Lundberg, 1995. Fig. 7). In some catfishes, the base of mental barbel bifurcates into an anterior (inner) ramus and a posterior (outer) ramus. In the Amblycipitidae, the tip of the posterior limb of the inner mental barbel is fused with the tip of the anterior limb of the outer mental barbel on the same side (Chen, 1994. Fig. 30; referred to as “anterior parts of cartilage contacting” by Diogo, 2005. P. 104). This feature was absent in the akysids examined by Chen (1994), but reported in *Glyptothorax*, *Glyptosternum* in the Sisoridae (Chen, 1994. Fig. 31b; Diogo et al., 2002. Fig. 5; Diogo, 2005. Fig. 3–121), and also in bagrid genera *Bagrus*, *Bagrichthys*, *Hemibagrus* (Diogo, 2005. Fig. 3–41). *Proliobagrus dorsalis* has such a “head-to-tail” fusion of the basal elastic cartilages (Figs. 11c, 12b). The similarity of fusion pattern of mental barbels may have independently evolved in amblycipitids, *Proliobagrus*, *Glyptothorax*, and *Glyptosternum*. Alternatively, the fusion of mental barbels may have been the plesiomorphic condition lost in akysids and some sisorids. The phylogenetic significance of this character in the Sisoroidea remains uncertain.

(5) Dorsoposterior expansion of jaw adductor muscle onto the skull roof (Chen, 1994. Fig. 14). In the Siluriformes, the jaw adductor muscle (adductor mandibularis muscle) usually attaches at the lateral margin of the skull roof, but has evolved to cover skull roof in some clades (Grande and Lundberg, 1988) by attaching at a “temporal fossa” formed by the sphenotic and pterotic, or further extending to an occipital transverse crest along the posterior margin of the skull. An anterior displacement of cranial exit of infraorbital canal from the sphenotic to the frontal is usually associated with such dorsoposterior expansion of the jaw adductor muscle (Grande and Lundberg, 1988). In the Amblycipitidae, this muscle largely covers the skull roof and reaches the occipital transverse crest (Chen, 1994). However, the site of cranial exit of infraorbital canal varies among amblycipitid genera, being the frontal in *Liobagrus* and *Xiurenbagrus* (Chen, 1994. Fig. 9; Chen and Lundberg, 1995. Fig. 4A; Sun, 2011. Fig. 4-1) but the anterior tip of the sphenotic in *Amblyceps* (Tilak, 1966. Fig. 1; Chen and Lundberg, 1995. Fig. 4B). In the Akysidae, the jaw adductor muscle attaches the lateral margin of skull roof. In the Sisoridae, no invasion of jaw adductor muscle on skull roof was reported. *Proliobagrus dorsalis* has the adductor muscle expanded on the skull roof and the infraorbital canal exiting from the frontal (Fig. 4a), a condi-

tion shared with *Liobagrus* and *Xiurenbagrus*. The inter-genus variation of cranial exit’s site of infraorbital canal in the Amblycipitidae may imply a homoplasy rather than a homology for the expansion of jaw adductor muscles onto skull roof among amblycipitid genera and *Proliobagrus*.

(6) Presence of an occipital transverse crest along posterior margin of skull roof (Chen, 1994. Figs. 9, 11; Chen and Lundberg, 1995. Fig. 4). The occipital transverse crest is developed for attaching epaxial muscles posteriorly, and jaw muscles anteriorly in the cases that jaw muscles cover the skull roof. Chen (1994) was the first to report the occipital transverse crest was present in the Amblycipitidae, but absent in the Akysidae and Sisoridae. However, our survey indicated that an occipital transverse crest is present on the supraoccipital of *Glyptosternum maculatum* (SWU 201909010179, SWU 201909020213), *Oreoglanis delacouri* (YU 20100514024) (Fig. 16b), *Oreoglanis immaculatus* (KIZ 200261018), *O. insignis* (KIZ 764025, KIZ 764447), *O. macropterus* (KIZ 740154), *Pseudencheneis sulcate* (KU 40671) and some other sisorid species. Thus, an occipital transverse crest is a derived character independently occurring in the Sisoroidea. Furthermore, as noted by Chen and Lundberg (1995), the occipital transverse crest develops on the supraoccipital alone in *Liobagrus* and *Xiurenbagrus* (Chen, 1994. Fig. 9; Chen and Lundberg, 1995. Fig. 4A), but on the supraoccipital and paired pterotics in *Amblyceps* (Chen, 1994. Fig. 11; Chen and Lundberg, 1995. Fig. 4B). This inter-genus variation among the Amblycipitidae may imply it as a homoplasy rather than a homology for amblycipitids. In *P. dorsalis*, an occipital transverse crest develops on the suproccipital alone which is similar to the condition in *Liobagrus* and *Xiurenbagrus* but different from that in *Amblyceps*.

In summary, our survey first suggested that the phylogenetic significance of three characters proposed by Chen (1994) is uncertain in the Sisoroidea: (1) the posterodorsal expansion of hyomandibula, (2) narrow posterodorsal intension of interopercle, and (3) fusion of the cartilaginous bases of inner and outer mental barbels. Second, the evident disparities between *Amblyceps* and (*Liobagrus + Xiurenbagrus*) related to three proposed synapomorphies: free margin of posterodorsal corner of the hyomandibula (gently convex vs. notched), the cranial exit site of infraorbital canal (on anterior tip of sphenotic vs. on frontal), location of occipital transverse crest (on supraoccipital + pterotic vs. on supraoccipital alone). Furthermore, our survey confirmed another osteological character disparity between *Amblyceps* and (*Liobagrus + Xiurenbagrus*) as noted by Chen and Lundberg (1995. Fig. 9), the bones bordering the foramen for facial nerve. In *Amblyceps*, this foramen is framed dorsally only by the pterosphenoid and ventrally by the parasphenoid, whereas in *Liobagrus + Xiurenbagrus* it is dorsally by the pterosphenoid and sphenoid, and ventrally by the parasphenoid. Our survey also indicated that, this

Table 1. Summary of morphological characteristics of *Proliobagrus dorsalis* in context of the Sisoroidea

Character type	Character status
Autapomorphies of <i>Proliobagrus</i>	Infraorbital bones reduced to the posteriormost element and lacrimal, first dorsal-fin pterygiophore anteriorly fused with a forward process, remote from the Weberian complex, compound Weberian centrum: an auxillary parapophysis posterolaterally off compound centrum, each half of fourth neural spine bifurcated dorsoventrally, presence of a ventral median ridge instead of paired ventrolateral ridges, anterior cranial fontanelle closed
Synapomorphies with the superfamily Sisoroidea	Posterior portion of autopalatine compressed and expanded vertically (de Pinna, 1996), articular region of lateral ethmoid elongated as process (de Pinna, 1996), a well-developed second ural centrum (de Pinna and Ng, 2014), bilobed swimbladder
Plesiomorphies in the Big Asia clade	First pectoral proximal radial roughly round (de Pinna, 1996), first dorsal-fin pterygiophore compressed, lacking paired bony canal for erector muscles
*Possible uniquely shared ones with the Amblycipitidae	The hyomandibula articulating with the lateral margin of the sphenotic, the supracleithrum is separated from the skull roof, and the posterolateral corner of the skull roof is only occupied by the pterotic
Possible uniquely shared ones with the Akysidae	Incomplete mesocoracoid arch (Mo, 1991)
Possible uniquely shared ones with the Akysidae and Sisoridae	Absence of claustrum (Mo, 1991)

* Based on our phylogenetic analysis including four amblycipitid species plus *Proliobagrus* (see discussion).

foramen framed by pterosphenoid + parasphenoid is present in all examined sisorid genera and species, whereas it is framed by pterosphenoid + sphenoid + parasphenoid in the all three examined akysid species *Acrochordonichthys rugosus*, *Akysis vespa*, *Pseudobagarius hardmani*.

A First Attempt at Phylogenetic Analysis

The superfamily Sisoroidea includes about 506 available species in three families (68 in the Akysidae, 54 in the Amblycipitidae, and 384 in the Sisoridae (Fricke et al., 2024). They are widely distributed, ranging from East Asia westwards to the Indian monsoon region and from Tibetan Plateau and adjacent mountains southwards to the Indo-Malaysian tropical region. We performed a detailed osteological study of *Proliobagrus*, but a thorough examination of character distribution among the Sisoroidea remains a challenge. On other hand, the previously proposed diagnostic characters for certain groups at various levels within the Sisoroidea also await thorough examination, which is beyond the scope of this study. For example, Chen and Lundberg (1995) proposed the characters to define clades within the Amblycipitidae in addition to the potential synapomorphies of this family, some of which await thorough revision. The 7-shaped endopterygoid used to be interpreted as a synapomorphy for Amblycipitidae + Akydidae + Parakysidae (now a subgroup within the Akysidae) is

variable in general shape (anteroposteriorly elongated vs. general shaped), while an elongated endopterygoid with “7” shape also present in *Bagarius yarrelli*. The posterolateral process of premaxilla is variable within *Liobagrus* (evident vs. absent) and between *Liobagrus* and *Amblyceps*, and the teeth are absent in this process in *Liobagrus* (Chen and Lundberg, 2015, Fig. 13c) but present in *A. yunnanensis* in our investigation. A hook-like process projecting anteriodorsally from dorsal margin of anterior ceratohyal is not observed in *X. gigas* in our investigation. Nevertheless, a first cladistic analysis of *Proliobagrus* was performed on the basis of a small sample size of sisoroids.

The cladistics analysis of the data matrix including the 66 osteological and one soft tissue, and one external morphological characters for 29 taxa (including three species representing three genera in the Akysidae, four species representing three genera in the Amblycipitidae, 13 species representing 12 genera in the Sisoridae) generated 15 equally parsimonious trees (tree length (L) = 221 steps, consistency index (CI) = 0.3439, retention index (RI) = 0.6771) that support the monophyly of the superfamily Sisoroidea, of the Akysidae, of the Sisoridae, and of the Amblycipitidae including *Proliobagrus* (Fig. 17). Relationships among the families of Sisoroidea are hypothesized as (Amblycipitidae, (Akysidae, Sisoridae)). In the majority rule consensus tree (Fig. 17b), the Amblycipitidae is split into two subclades. *Proliobagrus dorsalis* and *L. anguillicauda* are sister taxa, and *X. gigas* is sister to them,

whereas *A. mangois* and *A. yunnanensis* form the other one. Two characters are considered uniquely shared by this group: (1) the hyomandibula articulating with neurocranium through the lateral margin of the sphenotic instead of its ventral surface; (2) the supracleithrum is separated from the skull roof, and the posterolateral corner of the skull roof is only occupied by the pterotic. In the strict consensus tree (Fig. 17a), the relationships of species within the Amblycipitidae are unresolved except two *Amblyceps* species grouped together. Further investigations are warranted including more sisoroid taxa, especially those from genus *Amblyceps* and the Akysidae.

CONCLUSIONS

Subterranean waters provide a refuge for a few freshwater fishes over geological time (Muriel-Cunha, 2008; Babu, 2012; Vincent, 2012; Lundberg et al., 2014; Britz et al., 2014, 2018, 2020). *Proliobagrus* adds to the puzzle. Our osteological comparison and first phylogenetic analysis indicated that *Proliobagrus* is grouped with sampled amblycipitids, but it is distinguished from all known amblycipitid genera in a series of derived and plesiomorphic characters (Table 1). Thus, we suggest this subterranean catfish as a new genus within the superfamily Sisoroidea, and tentatively put it in the Amblycipitidae. In contrast to all known amblycipitid genera and species in which the first dorsal-fin pterygiophore wedging into posterior neural spines of the Weberian complex (neural spine of vertebra 4), *Proliobagrus* has a posteriorly placed dorsal fin which is far from the Weberian complex with the first dorsal-fin pterygiophore wedging into neural spines of vertebra 10. When and how this posteriorly placed dorsal fin evolves is interesting. Plesiomorphically in catfish, the first dorsal-fin pterygiophore inserts posterior to the posterior neural spine of the Weberian complex or the neural spines of vertebrae 5/6, and is adjacent to the Weberian complex. The evolution of posteriorly placed dorsal fin develops in some catfish groups, such as Heptapteridae catfish (Lundberg et al., 1991), Heptapterinae sensus (Silva et al., 2021), glyptosternines of the Sisoridae (Chu and Chen, 1990; Chu et al., 1999; Ng, 2015). The evolutionary trend is the gradually posteriorly placed from the neural spines of vertebra 4 or vertebrae 5/6 in the basal lineages to the more posterior positions, and apart from the Weberian apparatus, in the derived lineages (Silva et al., 2021, Fig. 1). The abrupt change of insert position of the first dorsal-fin pterygoid implies that none of extant amblycipitid species could be treated as the direct ancestor of *Proliobagrus*. If further analyses including more sampling species of *Amblyceps* and of the Akysidae from Southeast Asia support the putative familial assignment of *Proliobagrus* in this study, it will mean that its surface ancestor has been extinct and *Proliobagrus* represents a relic lineage surviving in subterranean waters of karst in South China. On other

hand, it would not be unexpected if alternative hypothesis is proposed for the origin of *Proliobagrus*. Further detailed all-genus morphology-based and molecular studies will finally establish the phylogenetic position of this enigmatic catfish, and this will be crucial for understanding the evolution history and diversification of the Asian superfamily Sisoroidea.

SUPPLEMENTARY INFORMATION

The online version contains supplementary material available at <https://doi.org/10.1134/S0032945224701017>

ACKNOWLEDGMENTS

Dr. You He appreciates Prof. Meeman Chang (Institute of Vertebrate Paleontology and Paleoanthropology, Chinese Academy of Sciences, Beijing, China) for motivating his curiosity about fish bones. We thank Dr. Guanghui Xu (Institute of Vertebrate Paleontology and Paleoanthropology, Chinese Academy of Sciences, Beijing, China), Dr. Huaqiao Zhang (Nanjing Institute of Geology and Palaeontology, Chinese Academy of Sciences, Nanjing, China) for their assistance in cladistic analyses using PAUP software. We thank Mr. Jiahu Lan (Du'an Fisheries Technology Extension Station, Du'an, China), Dr. Ziming Chen (Yunnan University, Kunming, China), Dr. Zuogang Peng (Southwest University, Chongqing, China), Dr. Deshou Wang (Southwest University, Chongqing, China), Mr. Shuwei Liu (Kunming Institute of Zoology, Chinese Academy of Sciences, Kunming, China), Dr. Xiaoyong Chen (Kunming Institute of Zoology, Chinese Academy of Sciences, Kunming, China), Dr. E. Zhang (Institute of Hydrobiology, Chinese Academy of Sciences, Wuhan, China) for loan specimens or permitting us examine the specimens under their care. We thank Dr. Gloria Arratia (University of Kansas, Lawrence, USA), Dr. Heok Hee Ng (National University of Singapore, Singapore), Dr. Neelesh Dahanukar (Shiv Nadar University, Delhi, India), Dr. Yaoguang Zhang (Southwest University, Chongqing, China), Dr. Haitao Zhao (Huaiyin Normal University, Huai-an, China), Dr. Wansheng Jiang (Kunming Institute of Zoology, Chinese Academy of Sciences, Kunming, China) for transferring the related literature.

FUNDING

This work was supported by National Natural Science Foundation of China (grants 31672250, 31860600).

ETHICS APPROVAL AND CONSENT TO PARTICIPATE

All applicable international, national, and/or institutional guidelines for the care and use of animals were followed.

CONFLICT OF INTEREST

The authors of this work declare that they have no conflicts of interest.

REFERENCES

- Arratia, G., Description of the primitive family Diplomystidae (Siluriformes, Teleostei, Pisces): morphology, taxonomy and phylogenetic implications, *Bonner Zool. Monograph.*, 1987, vol. 24, pp. 1–120.
- Arratia, G., The iluriform postcranial skeleton, in *Catfishes*, Enfield: Sci. Publ., 2003a, pp. 121–157.
- Arratia, G., Catfish head skeleton, *Ibid.*, 2003b, pp. 3–46.
- Arratia, G. and Huaquin, L., Morphology of the lateral line system and of the skin of diplomystid and certain primitive loricarioid catfishes and systematic and ecological considerations, *Bonner Zool. Monograph.*, 1995, vol. 36, pp. 1–110.
- Babu, K.S., *Horaglanis abdulkalami*, a new hypogean blind catfish (Siluriformes: Clariidae) from Kerala, India, *SAMGRA*, 2012, vol. 8, pp. 51–56.
- Birindelli, J.O. and Shibatta, O.A., Morphology of the gas bladder in bumblebee catfishes (Siluriformes, Pseudopimelodidae), *J. Morphol.*, 2011, vol. 272, pp. 890–896. <https://doi.org/10.1002/jmor.10961>
- Bockmann, F.A. and Castro, R.C., The blind catfish from the caves of Chapada Diamantina, Bahia, Brazil (Siluriformes: Heptapteridae): Description, anatomy, phylogenetic relationships, natural history, and biogeography, *Neotrop. Ichthyol.*, 2010, vol. 8, pp. 673–706. <https://doi.org/10.1590/S1679-62252010000400001>
- Britz, R., Kakkassery, F., and Raghavan, R., Osteology of *Kryptoglanis shajii*, a stygobitic catfish (Teleostei: Siluriformes) from Peninsular India with a diagnosis of the new family Kryptoglanidae, *Ichthyol. Explor. Freshwat.*, 2014, vol. 24, pp. 193–207.
- Britz, R., Sykes, D., Gower, D.J., et al., *Monopterus rong-saw*, a new species of hypogean swamp eel from the Khasi Hills in Northeast India (Teleostei: Synbranchiformes: Synbranchidae), *Ibid.*, 2018, vol. 28, pp. 315–326. <https://doi.org/10.23788/IEF-1086>
- Britz, R., Anoop, V.K., Dahanukar, N., et al., The subterranean *Aenigmachanna gollum*, a new genus and species of snakehead (Teleostei: Channidae) from Kerala, South India, *Zootaxa*, 2019, vol. 4603, pp. 377–388. <https://doi.org/10.11646/zootaxa.4603.2.10>
- Britz, R., Dahanukar, N., Anoop, V.K., et al., Aenigmachannidae, a new family of snakehead fishes (Teleostei: Channoidei) from subterranean waters of South India, *Sci. Rep.*, 2020, vol. 10, Article 16081. <https://doi.org/10.1038/s41598-020-73129-6>
- Carvalho, T.P., Reis, R.E., and Sabaj, M.H., Description of a new blind and rare species of *Xyliophius* (Siluriformes: Aspredinidae) from the Amazon Basin using high-resolution computed tomography, *Copeia*, 2017, vol. 105, pp. 14–28. <https://doi.org/10.1643/CI-16-456>
- Chardon, M., Parmentier, E., and Vandewalle, P., Morphology, development and evolution of the Weberian apparatus in Catfishes, in *Catfishes*, Enfield: Sci. Publ., 2003, pp. 71–120.
- Chen, X.P., Phylogenetic studies of the amblycipitid catfishes (Teleostei, Siluriformes) with species accounts, *Ph. D. Thesis*, Durham: Duke University, 1994.
- Chen, X.P. and Lundberg, J.G., *Xiurenbagrus*, a new genus of Amblycipitid catfishes (Teleostei: Siluriformes), and phylogenetic relationships among the genera of Amblycipitidae, *Copeia*, 1995, no. 4, pp. 780–800.
- Chu, X.L. and Chen, Y.R., *The Fishes of Yunnan, China*, Beijing: Sci. Press, 1990, pt 2.
- Chu, X.L., Zheng, B., and Dai, D., *Fauna Sinica, Osteichthyes, Siluriformes*, Beijing: Sci. Press, 1999.
- de Pinna, M.C., A phylogenetic analysis of the Asian catfish families Sisoridae, Akysidae, and Amblycipitidae, with a hypothesis on the relationships of the Neotropical Aspredinidae (Teleostei, Ostariophysi), *Fieldiana (Zool.)*, 1996, vol. 84, pp. 1–83.
- de Pinna, M.C. and Keith, P., *Mastiglanis durantoni* from French Guyana, a second species in the genus (Siluriformes: Heptapteridae), with a CT scan survey of phylogenetically-relevant characters, *Cybium*, 2019, vol. 43, pp. 125–135. <https://doi.org/10.26028/cybium/2019-423-002>
- de Pinna, M.C. and Ng, H.H., The second ural centrum in siluriformes and its implication for the monophyly of superfamily Sisoroidea (Teleostei, Ostariophysi), *Am. Mus. Novitates*, 2004, vol. 437, pp. 1–23.
- Devaere, S., Adriaens, D., Teugels, G.G., et al., Skeletal morphology of the holotype of *Gymnallabes nops* Roberts and Stewart, 1976, using micro CT-scanning, *Cybium*, 2005, vol. 29, pp. 281–293.
- Diogo, R., *Morphological Evolution, Adaptations, Homoplasies, Constraints, and Evolutionary Trends: Catfishes as a Case Study on General Phylogeny and Macroevolution*, Enfield: Sci. Publ., 2005.
- Diogo, R., Oliveira, C., and Chardon, M., On the osteology and myology of catfish pectoral girdle, with a reflection on catfish (Teleostei: Siluriformes) plesiomorphies, *J. Morphol.*, 2001, vol. 249, pp. 100–125. <https://doi.org/10.1002/jmor.1043>
- Diogo, R., Chardon, M., and Vandewalle, P., Osteology and myology of the cephalic region and pectoral girdle of *Glyptothonax fukiensis* (Rendahl, 1925), comparison with other sisorids, and comments on the synapomorphies of the Sisoridae (Teleostei: Siluriformes), *Belgian J. Zool.*, 2002, vol. 132, pp. 95–103.
- Diogo, R., Chardon, M., and Vandewalle, P., On the osteology and myology of the cephalic region and pectoral girdle of *Liobagrus reini* Hilgendorf, 1878, with a discussion on the phylogenetic relationships of the Amblycipitidae (Teleostei: Siluriformes), *Ibid.*, 2003, vol. 133, pp. 77–84.
- Dutra, G.M., Jerep, F.C., Vari, R.P., et al., The pseudotympanum in the Gymnotiformes (Teleostei, Ostariophysi, Otophysi): homology and evolution of a previously unexplored system in Neotropical electric fishes, *Zool. J. Linn. Soc.*, 2015, vol. 174, pp. 114–129. <https://doi.org/10.1111/zoj.12221>
- Fricke, R., Eschmeyer, W., and Fong, J., *Eschmeyer's Catalog Of Fishes, Version 10/2024*, 2024. <http://researcharchive.calacademy.org/research/ichthyology/catalog/SpeciesByFamily.asp>.

- Friel, J.P., A phylogenetic study of the neotropical banjo catfishes (Teleostei: Siluriformes: Aspredinidae), *Ph. D. Thesis*, Durham: Duke Univ., 1994.
- Gauba, R.K., Studies on osteology of Indidan Sisorid catfishes. 2. Skull of *Glyptothorax cavia*, *Copeia*, 1966, no. 4, pp. 802–810.
- Gauba, R.K., Studies on skull of Indian Sisoridae catfish *Erethistes pussilus*, *J. Zool.*, 1967, vol. 151, pp. 379–388.
- Gauba, R.K., On the morphology of the skull of catfish *Pseudecheneis sulcatus*, *Zool. Anzeiger*, 1968, vol. 181, pp. 226–236.
- Grande, L. and Lundberg, J.G., Revision and redescription of the genus *+Astrophus* (Siluriformes: Ictaluridae) with a discussion of its phylogenetic relationships, *J. Vertebrate Paleontol.*, 1988, vol. 8, pp. 139–171.
- He, S.P., The phylogeny of the Glyptosternoid fishes (Teleostei: Siluriformes, Sisoridae), *Cybium*, 1996, vol. 20, pp. 115–159.
- He, Y., Chen, X.Y., Xiao, T.Q., et al., Three-dimensional morphology of the *Sinocyclocheilus hyalinus* (Cypriniformes: Cyprinidae) horn based on synchrotron X-ray microtomography, *Zool. Res.*, 2013, vol. 34, pp. E128–134. <https://doi.org/10.11813/j.issn.0254-5853.2013.E4-5.E128>
- He, Y., Kim, B.J., Hirashima, K., et al., Skull and dentition of a hypogean goby *Luciogobius pallidus* revealed by synchrotron microtomography, *Cave Res.*, 2015, vol. 1, pp. 1–7.
- He, Y., Berra, T.M., and Wedd, D., A microtomographic osteology of the supraoccipital hook of nurseryfish, *Kurtus gulliveri* (Perciformes: Kurtidae), *Copeia*, 2016, vol. 106, pp. 897–906. <https://doi.org/10.1643/CI-15-365>
- He, Y., Chen, Y.X., Yang, J., et al., Phylogenetic analysis and osteological comparison of the cave-dwelling spined loach, *Bibarba parvoculus* (Cypriniformes: Cobitidae), and its surface congener, *Zool. J. Linn. Soc.*, 2021, vol. 191, pp. 1059–1074. doi: <https://doi.org/10.1093/zoolinnean/zlaa073>
- Kratochvil, H. and Ladich, F., Auditory role of lateral trunk channels in cobitid fishes, *J. Comp. Physiol. Sensory Neural Behav. Physiol.*, 2000, vol. 186, pp. 279–285. <https://doi.org/10.1007/s003590050428>
- Kubicek, K.M., Developmental osteology of *Ictalurus punctatus* and *Noturus gyrinus* (Siluriformes: Ictaluridae) with a discussion of siluriform bone homologies, *Vertebrate Zool.*, 2022, vol. 72, pp. 661–727. doi: <https://doi.org/10.3897/vz.72.e85144>
- Lundberg, J.G., The evolutionary history of North American catfishes, family Ictaluridae, *Ph. D. Thesis*, Ann Arbor: Univ. of Michigan, 1970.
- Lundberg, J.G., The comparative anatomy of the toothless blindcat, *Trogloglanis pattersoni* Eigenman, with a phylogenetic analysis of the Ictalurid Catfishes, *Misc. Publ. Mus. Zool., Univ. Michigan*, 1982, vol. 163, pp. 1–85.
- Lundberg, J. G. and Baskin, J.N., The caudal skeleton of the Catfishes, order Siluriformes, *Am. Mus. Novit.*, 1969, vol. 2398, pp. 1–49.
- Lundberg, J.G., Bornbusch, A.H., and Mago-Leccia, F., *Gladioglanis conquistator* n. sp. from Ecuador with diagnoses of the subfamilies Rhamdiinae Bleeker and Pseudopimelodidae n. subf. (Siluriformes: Pimelodidae), *Copeia*, 1991, pp. 190–209. <https://doi.org/10.2307/1446263>
- Lundberg, J.G., Luckenbill, K.R., Babu, K.S., et al., A tomographic osteology of the taxonomically puzzling catfish *Kryptoglanis shajii* (Siluriformes, Siluroidei, incertae sedis): Description and a first phylogenetic interpretation, *Proc. Acad. Nat. Sci. Philadelphia*, 2014, vol. 163, pp. 1–41.
- Lundberg, J.G., Hendrickson, D.A., Luckenbill, K.R., et al., Satan's skeleton revealed: A tomographic and comparative osteology of *Satan eurystomus*, the subterranean Wide-mouth Blindcat (Siluriformes, Ictaluridae), *Ibid.*, 2017, vol. 165, pp. 117–173. <https://doi.org/10.1635/053.165.0108>
- Mahajan, C.L., *Sisor rhabdophorus*—A study in adaptation and natural relationship. I. Head skeleton, *J. Zool.*, 1966, vol. 149, pp. 365–393.
- Mahajan, C.L., *Sisor rhabdophorus*—A study in adaptation and natural relationship. 3. Vertebral column median fins and their musculature, *Ibid.*, 1967, vol. 152, pp. 297–318.
- Mo, T.P., Anatomy, relationships and systematics of the Bagridae (Teleostei, Siluroidei) with a hypothesis of siluroid phylogeny, *Theses Zool.*, 1991, vol. 17, pp. 1–216.
- Muriel-Cunha, J., Biodiversidade e sistemática molecular de Phreatobiidae (Ostariophysi, Siluriformes)—com uma proposta sobre sua posição filogenética em Siluriformes e uma discussão sobre a evolução do hábito subterrâneo, *Ph. D. Thesis*, São Paulo: Universidade de São Paulo, 2008.
- Ng, H.H., The monophyly and composition of the Asian hillstream catfish family Sisoridae (Teleostei: Siluriformes): Evidence from morphology, *Ichthyol. Explor. Freshw.*, 2010, vol. 21, pp. 247–278.
- Ng, H.H., Phylogenetic systematics of the Asian catfish family Sisoridae (Actinopterygii: Siluriformes), *Ibid.*, 2015, vol. 26, pp. 97–157.
- Ng, H.H. and Jiang, W.S., Intrafamilial relationships of the Asian hillstream catfish family Sisoridae (Teleostei: Siluriformes) inferred from nuclear and mitochondrial DNA sequences, *Ibid.*, 2015, vol. 26, pp. 229–240.
- Ng, H.H. and Kottelat, M., *Pterocryptis buccata*, a new species of catfish from western Thailand (Teleostei: Siluridae) with epigean and hypogean populations, *Ichthyol. Res.*, 1998a, vol. 45, pp. 393–399. <https://doi.org/10.1007/BF02725192>
- Ng, H.H. and Kottelat, M., The catfish genus *Akysis Bleeker* (Teleostei: Akysidae) in Indochina, with descriptions of six new species, *J. Nat. History*, 1998b, vol. 32, pp. 1057–1097. <https://doi.org/10.1080/00222939800770531>
- Ng, H.H. and Kottelat, M., *Parakysis notialis*, a new species of akysid catfish from Borneo (Siluriformes: Akysidae), *Ichthyol. Res.*, 2003, vol. 50, pp. 48–51. <https://doi.org/10.1007/s102280300006>
- Ng, H.H. and Ng, P.L., A revision of the akysid catfish genus *Acrochordonichthys* Bleeker, *J. Fish Biol.*, 2001, vol. 58, pp. 386–418. <https://doi.org/10.1111/j.1095-8649.2001.tb02260.x>
- Nixon, K. C., *WinClada*, Version 1.00.08, 2002, <http://www.cladistics.com>.
- Ohara, W.M., Da Costa, I.D., and Fonseca, M.L., Behaviour, feeding habits and ecology of the blind catfish *Phreatobius sanguijuela* (Ostariophysi: Siluriformes), *Ibid.*, 2016, vol. 89, pp. 1285–1301. <https://doi.org/10.1111/jfb.13037>

- Proudlove, G.S., Biodiversity and distribution of the subterranean fishes of the World, in *Biology of Subterranean Fishes*, Trajano, E., Eds., Enfield: Sci. Publ., 2010, pp. 41–64.
- Rizzato, P.P. and Bichuette, M.E., The laterosensory canal system in epigean and subterranean *Iuglanis* (Siluriformes: Trichomycteridae), with comments about troglomorphism and the phylogeny of the genus, *J. Morphol.*, 2017, vol. 278, pp. 4–28.
<https://doi.org/10.1002/jmor.20616>
- Roberts, T., *Ayarnangra estuaricus*, a new genus and species of Sisorid catfish from the Ayeyarwaddy basin, Myanmar, *Nat. History Bull. Siam Soc.*, 2001, vol. 49, pp. 81–87.
- Rodiles-Hernandez, R., Hendrickson, D.A., Lundberg, J.G., et al., *Lacantunia enigmatica* (Teleostei: Siluriformes) a new and phylogenetically puzzling freshwater fish from Mesoamerica, *Zootaxa*, 2005, vol. 1000, no. 1, pp. 1–24.
<https://doi.org/10.11646/zootaxa.1000.1.1>
- Romero, A. and Paulson, K., It's a wonderful hypogean life: A guide to the troglomorphic fishes of the world, *Environ. Biol. Fish.*, 2001, vol. 62, pp. 13–41.
<https://doi.org/10.1023/A:1011844404235>
- Sabaj, M.A., Codes for natural history collections in ichthyology and herpetology, *Copeia*, 2020, vol. 108, pp. 593–669.
<https://doi.org/10.1643/ASIHCODONS2020>
- Schaefer, S.A., Relationships of *Lithogenes villosus* Eigenmann, 1909 (Siluriformes, Loricariidae): Evidence from high-resolution computed microtomography, *Am. Mus. Novitates*, 2003, vol. 3401, pp. 1–55.
- Shibatta, O.A., Muriel-Cunha, J., and de Pinna, M.C., A new subterranean species of *Phreatobius Goeldi*, 1905 (Siluriformes, Incertae sedis) from the Southwestern Amazon basin, *Papéis Avulsos de Zoologia (São Paulo)*, 2007, vol. 47, pp. 191–201.
<https://doi.org/10.1590/S0031-10492007001700001>
- Silva, G.C., Roxo, F. F., Melo, B. F., et al., Evolutionary history of Heptapteridae catfishes using ultraconserved elements (Teleostei, Siluriformes), *Zool. Scripta*, 2021, vol. 50, pp. 543–554.
<https://doi.org/10.1111/zsc.12493>
- Sullivan, J.P., Lundberg, J.G., and Hardman, M., A phylogenetic analysis of the major groups of catfishes (Teleostei: Siluriformes) using rag1 and rag2 nuclear gene sequences, *Mol. Phylogen. Evol.*, 2006, vol. 41, pp. 636–662.
<https://doi.org/10.1635/053.162.0106>
- Sullivan, J.P., Peng, Z.G., Lundberg, J.G., et al., Molecular evidence for diphyley of the Asian catfish family Amblycipitidae (Teleostei: Siluriformes) and exclusion of the South American Aspredinidae from Sisoroidea, *Proc. Acad. Nat. Sci. Philadelphia*, 2008, vol. 157, pp. 51–65.
[https://doi.org/10.1635/0097-3157\(2008\)157\[51:MEF-DOT\]2.0.CO;2](https://doi.org/10.1635/0097-3157(2008)157[51:MEF-DOT]2.0.CO;2)
- Sun, Z., Systematic taxonomy of Chinese mainland species of the amblycipitid catfish genus *Liobagrus* Hilgendorf, 1878, *Master's Thesis*, Wuhan: Inst. Hydrobiol., Chinese Acad. Sci., 2011.
- Swofford, D.L., PAUP—A computer-program for phylogenetic inference using maximum parsimony, *J. Gen. Physiol.*, 1993, vol. 102, pp. A9–A9.
- Tilak, R., The osteocranum and Weberian apparatus of the fishes of the family Sisoridae (Siluroidea): A study in adaptation and taxonomy, *Zeitschrift Wissenschaft. Zool. (Leipzig)*, 1963, vol. 168, pp. 281–320.
- Tilak, R., The osteocranum and the Weberian apparatus of the fishes of the family Bagridae (Pisces: Siluroidei), *Gegenbaurs Morphol. Jahrbuch* (Leipzig), 1965, vol. 107, pp. 415–443.
- Tilak, R., The osteocranum and Weberian apparatus of *Amblyceps mangois* (Hamilton) (Pisces: Siluroidei) in relation to taxonomy, *Zool. Anzeiger*, 1967, vol. 178, pp. 61–74.
- Vincent, M., Occurrence, distribution and troglomorphisms of subterranean fishes of peninsular India, *Curr. Sci.*, 2012, vol. 102, pp. 1028–1034.
- Vishwanath, W., Darshan, A., and Anganthoibi, N., Osteology of some catfishes of the genus *Glyptothorax* (Teleostei: Siluriformes) of northeastern India, *J. Threatened Taxa*, 2010, vol. 2, pp. 1245–1250.
- Xiu, L.H., Yang, J., and Zheng, H.F., An extraordinary new blind catfish, *Xiurenbagrus dorsalis* (Teleostei: Siluriformes: Amblycipitidae), from Guangxi, China, *Zootaxa*, 2014, vol. 3835, pp. 376–380.
<https://doi.org/10.11646/zootaxa.3835.3.7>
- Zhang, Y.G. and Wang, D.S., Studies on the osteology of the bagrid catfishes from the Jialing river. I. Comparison of the Weberian apparatus, *J. Southwest China Normal Univ. (Nat. Sci.)*, 1995, vol. 20, pp. 53–58.
- Zhang, Y.G., Wang, D.S., and Pu, D.Y., Studies on the osteology of the bagrid catfishes from the Jialing river. III. Comparison of the skulls, *Ibid.*, 1995, vol. 20, pp. 285–292.
- Zhou, W. and Zhou, Y.W., Phylogeny of the genus *Pseudocheneis* (Sisoridae) with an explanation of its distribution pattern, *Zool. Stud.*, 2005, vol. 44, pp. 417–433.

Publisher's Note. Pleiades Publishing remains neutral with regard to jurisdictional claims in published maps and institutional affiliations. AI tools may have been used in the translation or editing of this article.